RC1 comments,

1. Introduction

- From my understanding, the EOG and the EWS are not thrown out in the 4th edition but the standard has been expanded. This should be clarified.
- Ans: This is correct. We have addressed this in text (line 35 in marked-up version)
- The wind speed information you are giving in l. 74 is not accurate. If you are bringing up the specific values, you should explain what the values you are just citing here actually mean - not a normal inflow velocity of 50 m/s but the reference wind speed (for the definition, please look into IEC-61400-1 4th edition)
- Ans: clarification has been added (Line 79 in marked-up version)
- While you are now citing the 3rd and 4th edition of the IEC 61400-1 standard, you are using the formulas of the 2nd version (at least, I suppose you do since you did not change the formulas). Change the formulas or the citation. Do not use wrong citations.
- Ans: True! it was a mistake and all the equations and figures have been addressed according to 3rd version. Thank you for this!
- the authors should point our why the gust slicing effect is a problem (recurring high loads while the turbine blade crosses the gust several times)
- Ans: this has been added in line 49 in marked-up version. Thank you!

2. Methodology

2.1. windEEE dome

- in the text, both figure 2a and figure 2b are said to show "the closed-circuit 2D ow mode" while the caption says "render of test chamber and ow path" (a) and "side view schematic of the WindEEE Dome with ow path in closed-circuit straight ow mode" (b). Please clarify the description. Do I interpret the figures correctly when saying that the flow returns around the inner chamber (i.e. left, right, above)?
- Ans: this has been addressed now as figure 1. The flow just recirculates from top, the surrounding part of the outer shell are isolated from the fans' suction side with special sealed doors in 2D flow mode. The figure has been reconfigured accordingly.
- you are mentioning the repeatability of gusts and shear flows. I would like to know whether this has been shown somewhere and if a citation could be included.
- Ans: we have not done any repeatability study on the produced gusts yet, as now specified in manuscript (line 219 in marked-up version); we tried various actuating time for fans and IGVs then processed the data and selected the best configurations for which the results are presented. In order to recognize this we deleted the word "repeatable" in line 148 even though the gusts from IGVs look consistently identical (figure 11f & g).

2.2. Numerical Flow Analysis Setup and Tuning/Validation

- In this part, you should be clear about using one static condition to validate the numerical setup while the numerical setup will afterwards be used dynamically to generate the gusts and the shear. This could also be used in the discussion of the deviation in the flow field due to the different performance in the upper fan rows (as you write, "By knowing these discrepancies, corrections can be applied to the fan inputs").

- Ans: This has been added in the manuscript, thank you! Line 204, 310.

2.3. Gust length and time scaling

- I could not find any reference of the 14s duration of the 50 year EOG in the IEC 61400-1 ed 3 and 4 standards, could you please give me the section where I can find this?
- Ans: That was based on second version, it has been addressed in line 228 and other relative sections and figures.
- (question out of interest): with a TSR of 1.1 and an inflow velocity of 5 m/s, the rotational frequency of the turbine (R = 1.1m) would be less than 1Hz which appears very slow to me. Is there a mistake?
- Ans: True: the RPM will be around 56. To capture the effect of the 5 s gust on the turbine and being able to relate it to the full scale based on our assumption that should be the operational TSR for a future experiment that would include the turbine.
- It is not clear what you want to express here. Please rephrase this.
- Ans: it has been rephrased in Line 263. This part presents the assumptions for the parameters that affect the profile of the extreme events. the full scale and scaled extreme condition figures have been moved together in this section.

3. Results and discussion

3.1. Steady wind shear

- I would change the wording in line 263: you are talking about velocity deviations, but the standard deviation gives you a measure of the fluctuations in the flow

- Ans: it has been addressed in line 298.

- it is not clear what the setting of 1.6 s is and what it implies. If the information is relevant, please be more specific.

- Ans: explanation has been added in line 323.

- I do not agree with the use of the term "intermittency" in this context because in turbulence, it is normally used for effects occurring in the ow due to the turbulence while here, in contrast, the short, strong dip in the velocity is not caused by turbulence but more likely due to the setup. I suggest rephrasing the explanation.

- Ans: Different wording has been used in lines 362 and 364.

- A thought regarding the velocity "dip": When looking at the time series, it is obvious that the higher measurement positions have higher turbulence levels and in addition, probe H measures this "dip" - could this be explained by the upper fans having a less stable air supply than the lower fans who will suck more air from the sides and above? (due to the sharp angle between the upper row of the fans and the plenum, I would expect more air to ow from there to the lover fans) And could this dip be related (lack of air when suddenly increasing the velocity)?

- Ans: That is overall correct. The upper fans have less supply due to the sharp angle. However, this effect has been minimized in WindEEE by installing returning vanes at the top of the outer circuit. We have now commented on this aspect in line 363 in marked up version.

4. Conclusion

- While you are talking about a "numerical and experimental study" both in your title and the discussion, I do not feel that this is an accurate description since you are describing how you build a numerical "setup-preparation chain" that you validate against previous ABL data sets, and this numerical setup is in the following used to set the vans. However, you are not showing the simulation results of the gusts and shears, and therefore it is not directly a numerical study in my opinion. What you compare are the experimental results and the expected results from the formulas. I therefore think it would aid if you would rephrase the first sentence of the conclusion. Is a numerical study with a simulation and experimental campaign for example with the turbine planned in the future?
- Ans: line 381 has been modified to recognize this. The intent going forward is indeed to be able to compare simulation to experiment.
- "The steady experiment runs corresponding to the peak of the shear cases show the fans act non-linearly and they have different individual efficiencies, especially the top and bottom rows despite our simplified assumptions for developing the CFD model." I would suggest rephrasing: "The steady experiment runs corresponding to the peak of the shear cases show THAT the fans act non-linearly and THAT they have different individual efficiencies, especially the top and bottom rows. This has not been taken into account in our simplified assumptions for developing the CFD model."
- Ans: thank you, line 415 has been modified.

5. Referee comments

- It would have been nice if specific information (for example the lines) on the changes that have been made in response to the reviewers' comments would have been added.
- Ans: Thank you for noting that, we have tried to highlight the corresponding line to the modifications made in the marked-up version along with the line numbers that are included here.
- When asking about a) the phase average of your gust and b) the repeatability, comment on fig. 12, I wanted to know whether you repeated the experiment several times and checked a) whether the gust events are similar and b) whether the plots are presenting an average over multiple gusts. I did understand that you use a filtering with a 0.2s moving average but this is not a phase average. Could you please clarify the above-mentioned points and add this in the paper? I could not find the information that the cobra probes show variations in the measurement of the mean velocity in the revised paper.
- Ans: The plots have not been phase averaged based on multiple experiment runs. They are just showing one individual experiment run as now specified in manuscript (line 219 in marked-up

version). We tried various actuating time for fans and IGVs then processed the data and selected the best configurations for which the results are presented. In order to recognize this we deleted the word “repeatable” in line 148 even though the gusts from IGVs look consistently identical (figure 11f & g). A study on the reproducibility has been recommended for future work (line 415). The velocity variations due to the filtering has been added in line 339.

RC2 Comments,

1. **Referee comments**

- Numerical Analysis. Please specify `surface curvature, surface growth rate and mesh density were left to default values' in the revised manuscript.
- Ans: they have been added in line 169 in marked-up version
- Exp. details. The added paragraph `The seven cables from all the cobra probes....to digital converter card' does not address my comment. This section still lacks actual details necessary for repeatability purposes. Please add those in your next review.
- Ans: as has been added in line 219, no repeatability investigation has been done yet. Because we did not know how to modulate the actuating time of the power and IGVs, a set of experiments with different timing were run. We selected the best configurations for which the results are presented. In order to recognize this we deleted the word "repeatable" in line 148 eventhough the gusts from IGVs look consistently identical (figure 11f & g).
- Results. Please include some form of your reply to my question on `error exist in horizontal shear'.
- Ans: it has been added in line 310.

2. **Further comments**

- abstract - I suggest replacing `proper' with `appropriate'.
- Ans: addressed at line 18.
- page 2, 65 - I suggest replacing `cause' with `can cause'.
- Ans: addressed at line 48
- page 2, 65 - I suggest replacing `All these together' with `All these phenomena together'.
- Ans: addressed at line 67.
- page 3, 95 - I suggest replacing `This standard' with `The ICE'.
- Ans: addressed at line 73
- page 4, 111 - I suggest replacing `at figure 1' with `in figure 1'.
- Ans: it has been addressed through the manuscript
- figure 3 - I do not see what this figure adds to the manuscript. I would suggest removing it altogether.
  Ans: Thank you for your comment but the gusts with IGVs had the best results; we feel a small presentation of them helps the audience to understand their function.
- page 12, 235 - I suggest replacing `According to Figure 5a &b showing the relative errors between velocities at each height, the largest disconformities....' with `Figure 5a &b show the relative errors between velocities at each height. The largest disconformities....'
- Ans: thank you! It has been changed in line 195.

- page 12, 245 - I suggest replacing `at figure 6' with `in figure 6'. Please rephrase this throughout the manuscript.
- Ans: this has been done, thanks.
- page 16, 300 - The mismatch in Re is substantial, which is understandable. The authors should limit their discussion on convincing their audience that this is not a strong limiting factors of their work, rather than including general statements on how to increase the Re.
- Ans: It has been moved to line 282.
- figure 9 - I remain convinced that figures 1 and 9 should be collated. The blue line can be described at first, then the dashed red line discussion can be left to page 18.
- Ans: They have been moved together as figure 8 in section 2.4. thank you!
- page 19, 345 - This sentence is unclear. I suggest rephrasing it for clarity.
- Ans: it has been addressed in line 307.
- page 21, 355 - This sentence is unclear. I suggest rephrasing it for clarity.
- Ans: it has been addressed in line 321.
- page 24, 395 - I suggest replacing `As mentioned earlier' with `As previously discussed'.
- Ans: it has been addressed in line 358.
- page 24, 395 - The first sentence starting with `However' is unclear. I suggest rephrasing it for clarity.
- Ans: it has been addressed in line 362.
- page 28, 405 - I suggest replacing `with the theory' with `to the theory'.
- Ans: it has been addressed in line 379.
- figures 12&13 - The authors insist on not discussing all subfigures, although these are now at least introduced. I have already pointed out that this is far from best practice.
- Ans: figure 12 now as 11, it is just showing the total time history related to the whole experiment, we have tried to add more discussion about this figure. Figure 13 now as 12, which is more detailed; we have added to our discussion in lines 360 to 376 to this section. Thank you for your constructive comments.
- My concern regarding the lack of a well-structured conclusion section to this work has not been fully addressed. I will not recommend publication of this manuscript without substantial improvements to this section. E.g. page 29, 420 - The first paragraph needs rephrasing for clarity.
- Ans: the conclusion has been restructured and improved.
- Page 29, 420 - When the authors say `despite our simplified assumptions for developing the CFD model', do they mean `which highlights the limitations of our idealised CFD modelling'?
- Ans: Yes! That sentence has been rephrased.
- Page 29, 425 - The authors state `...more distorted...'. What does this refer to?
- Ans: It was rephrased in Line 418. By distortion I meant the time lag between the high and the low peak hitting the test section.
- Please do review the conclusion.
- Ans: We restructured the conclusion.

~~Numerical and~~ Experimental and Numerical Simulation of Extreme Operational Conditions for Horizontal Axis Wind Turbines Based on the IEC Standard

Kamran Shirzadeh [1,2], Horia Hangan [1,3], Curran Crawford [1,4]

[1] WindEEE Research Institute, University of Western Ontario, London, Ontario, N6M 0E2, Canada
[2] Mechanical and Material Engineering, Western University, London, N6A 3K7, Canada
[3] Civil and Environment Engineering, Western University, London, N6A 3K7, Canada
[4] Mechanical Engineering, Victoria University, Victoria, V8W 2Y2, Canada

Correspondence: Kamran Shirzadeh (kshirzad@uwo.ca)

Abstract. In this study, the possibility of simulating some transient and deterministic extreme operational conditions for horizontal axis wind turbines based on the IEC 61400-1 standard using 60 individually controlled fans in the Wind Engineering, Energy and Environment (WindEEE) Dome at Western University was investigated. Experiments were carried out for the Extreme Operational Gust (EOG), positive and negative Extreme Vertical Shear (EVS), and Extreme Horizontal Shear (EHS) cases, tailored for a scaled 2.2 m horizontal axis wind turbine. For this purpose, firstly a numerical model for the test chamber was developed and used to obtain the fans' configurations for simulating each extreme condition with ~~proper~~appropriate scaling prior to the physical experiments. The ~~result shows~~results show the capability of ~~the developed~~using numerical ~~model~~modeling to predict the fans' setup ~~and the facility to~~based on which physical simulations can generate IEC extreme conditions in the range of interest.

1. Introduction

Wind energy is one of the primary sources of renewable ~~energies~~energy for ~~mitigating~~mitigation of the ~~global~~ increasing global energy demand. However, one of the basic factors for this market to thrive is a continued ~~lowering~~decline of the levelized cost of electricity (LCOE), which is enhanced by ensuring the life time of the wind energy systems is reliably long (Ueckerdt et al., 2013). Having a long life cycle for these energy systems dramatically increases the probability of them encountering various extreme weather and wind conditions. Therefore, the design of wind energy systems must consider extreme environmental conditions with statistically accurate return periods. The International Electrotechnical Commission (IEC) has some deterministic design codes for commercial Horizontal Axis Wind Turbines (HAWT) in operating conditions, specifically in the third edition of the IEC 61400 part one (IEC, 2005) ~~which includes two return periods for extreme conditions during turbine operation, 1 and 50 years.~~. These extreme models are relatively simple and are not able to capture the true coherent turbulent wind characteristics (Cheng and Bierbooms, 2001; Hansen and Larsen, 2007; Wächter et al., 2012). This is especially true in complex terrain where the gust time evolution profiles are highly asymmetric and non-Gaussian (Hu et al., 2018). It has also motivated the most recent edition of the IEC standard (IEC, 2019) to utilize statistical methods for characterizing extreme gust event performance and extrapolation of load cases. This has been enabled by computational resources to analyse wind energy systems in dynamic wind environments~~.~~ to expand their external condition models. However, the third edition of the IEC standards was used in the work presented here as an initial step towards gust experimentation and represents an incremental development of a gust loading experimental capability. Progressing to a stochastic experimental approach, ~~in order to replicate the much more complex current standard aimed at numerical simulation efforts,~~ is left for future work and will be very challenging.

One of the extreme cases in the standard is the extreme operational gust (EOG). A gust is defined as a sudden increase in velocity over its mean value, which is a transient feature of a turbulent wind field (Burton et al., 2011).These turbulent features in the Atmospheric Boundary Layer (ABL) depend on topography, surface roughness, up-stream obstacles, thermal stability (Suomi et al., 2013) and mesoscale climactic systems such as thunderstorms and downbursts (Chowdhury et al., 2018). In theory for different ~~application~~applications, there are various simplified models of gust based on a peak factor and the whole rising and falling time in the wind speed. The peak factor is the ratio of the peak velocity (maximum or minimum) and the average wind speed. Wind gusts can happen over various length and time scales in nature. The most damaging gusts for any type of structures are the ones that have the same length scale as the structure that can envelope the whole structure (Hu et al., 2018). Smaller gusts, relative to ~~the~~ wind turbine size~~, cause fatigue loads on blades and~~ can induce dynamic stall and the gust slicing effect (i.e. ~~a~~ recurring high loads as the blade slices through the spatial/temporal gust ~~repeatedly as it rotates~~region several times). The wind gusts also can cause intermittencies in the power output of wind turbine generators. For a small electricity network, these fluctuations in power generation can cause serious problems (e.g. unstable grid voltage and frequency) for managing power transmission and distribution (Anvari et al., 2016; Estanqueiro, 2007). The worst case in both terms of the grid stability and the loading on the turbine is when the gust peak speed is higher than the wind turbine cut-out speed (i.e. a specific speed that turbine comes to complete parked position for safety reasons, usually about 25 m/s), which if prolonged enough can cause the control system to abruptly stop the wind turbine (Hansen, 2015). From an aerodynamic point of view, gusts can result in undesired acceleration of the rotor and drivetrain. The most reasonable solution is usually an adjustable generator load or ~~adjusting~~ blade pitch angles after detection of the gust for modern wind turbines (Pace et al., 2015; Lackner and Van Kuik, 2010). Developing LIDAR technology can make a substantial contribution in controlling the wind turbine by measuring the wind field upstream, thereby giving enough time for the control system to react properly (Bossanyi et al., 2014; Schlipf et al., 2013).

In addition to uniform gusts, the standard specifies deterministic Extreme Vertical and Horizontal Shears (EVS, EHS). These Extreme Wind Shears (EWS) can induce asymmetric loads on the rotor which are in turn transferred into the whole structure. The vertical shears can induce tilting or out-of-plane moments on the rotor and nacelle (Micallef and Sant, 2018). In a positive vertical shear, the blade moving at higher heights could experience stall while the one moving at lower height will experience a reduction in overall angle of attack relative to design condition (and vice versa for negative vertical shear) (Sezer-Uzol and Uzol, 2013). If the shear is extreme enough, the blades may experience a phenomenon known as dynamic stall (Hansen, 2015; Gharali and Johnson, 2015). All these phenomena together will result in high fluctuations in power generation, as well as highly dynamic fatigue loads on the structure (Jeong et al., 2014; Shen et al., 2011). The effects of horizontal shear are similar to vertical shear in terms of power performance and blade fatigue loads. However, EHS also induces yaw moments. These transient shears can happen for similar reasons as uniform gusts, but mostly happen within wind farms, where the downstream wind turbines are partially exposed to the wakes of other operating turbines (González-Longatt et al., 2012; Thomsen and Sørensen, 1999).

~~This standard also~~The IEC defines a classification for commercial wind turbines based on a reference wind speed and turbulence intensity, in a way that covers most on-shore applications (IEC, 2005). The Turbulence Intensity (TI) is defined as the ratio of the standard deviation of wind speed fluctuations to the average wind speed both calculated in ~~10min~~10 min intervals. TI levels of 16%, 14% and 12% ~~correspond~~corresponding to the A, B and C ~~the~~ reference turbulence classes (I_{ref}). For velocity references~~,~~ (U_{ref}), 3 classes have been defined (I, II, III) ~~corresponding to~~ with 50, 42.5, 37.5 m/s as reference wind speeds, with one further class for special conditions (e.g. offshore and tropical storms) which should be specified by the designer. These reference velocities are used to calculate parameters related to the turbine external conditions. For example, the standard mean value of the wind speed over a 10 min interval based on the turbine class is $0.2\ U_{ref}$. An extreme wind speed model as a function of height (Z) respect to the hub height (Z_{hub}) with recurrence period of 50 years (U_{e50}) and 1 year (U_{e1}), is defined as follows:

$$U_{e50}(z) = 1.4U_{ref}\left(\frac{Z}{Z_{hub}}\right)^{0.11},$$
$$U_{e1}(z) = 0.8U_{e50}(z), \qquad (1)$$

This definition is used for calculating the gust magnitude of the EOG.

The design stream-wise turbulence standard deviation (σ_u) is defined by a normal turbulence model:

$$\sigma_u = I_{ref}(0.75U_{hub} + b); \quad b = 5.6\ \frac{m}{s}, \qquad \cancel{(1)}\ (2)$$

Formatted Table

The U_{hub} is the average wind velocity at the at hub-height and b is a constant. Accordingly, the hub height gust magnitude (U_{gust}) is given as:

$$U_{gust} = min\left\{1.35(U_{e1} - U_{hub}); 3.3\left(\frac{\sigma_u}{1+0.1\left(\frac{D}{\Lambda_u}\right)}\right)\right\}, \qquad (3)$$

Considering t as the instantaneous time and $t = 0$ ~~at~~as the beginning of the gust, the uniform EOG as function of time is defined as:

$$\cancel{U(t) = \begin{cases} \overline{U_{hub}} - 0.37\beta\left(\frac{\sigma_u}{1+0.1\left(\frac{D}{\Lambda_u}\right)}\right) sin\frac{3\pi t}{T}\left(1-cos\frac{2\pi t}{T}\right); when \quad 0 \le t \le T, \\ \overline{U_{hub}}; \quad when\ t > T\ or\ t < 0, \end{cases}} \quad U(t) \qquad \cancel{(2)}$$

$$= \begin{cases} \overline{U_{hub}} - 0.37U_{gust}\, sin\frac{3\pi t}{T}\left(1-cos\frac{2\pi t}{T}\right); when \quad 0 \le t \le T, \\ \overline{U_{hub}}; \quad when\ t > T\ or\ t < 0, \end{cases} \qquad (4)$$

The ~~factor β takes~~ T is the ~~value of 4.8 or 6.4 for gusts with recurrence periods of 1 or 50 years respectively. The~~ duration of the gust ~~T is~~, specified as 10.5 ~~s for 1-year and 14 s for 50-years return periods~~seconds. The D is the diameter of the rotor, and Λ_u is the longitudinal turbulence scale parameter which is a function of the hub height ~~(Z_{hub}):~~:

$$\Lambda_u = \begin{cases} 0.7Z_{hub} & for\ Z_{hub} \le 60\ m, \\ 42m & for\ Z_{hub} > 60\ m, \end{cases} \qquad \cancel{(3)}\ (5)$$

The EVS and EHS have similar equations ~~which~~that can be added to or subtracted from the main uniform or ABL inflow. The EVS as function of height ~~(Z)~~ and time can be calculated using the ~~Eq.~~equation ~~(4):~~(6).

$$U_{EVS}(Z,t) = \begin{cases} \left(\frac{Z - Z_{hub}}{D}\right)\left(2.5 + 0.2\,\beta\sigma_u\left(\frac{D}{\Lambda_u}\right)^{0.25}\right)\left(1 - \cos\left(\frac{2\pi t}{T}\right)\right); when \quad 0 \le t \le T, \\ 0 \quad ; when\ t > T\ or\ t < 0, \end{cases} \qquad \cancel{(4)}\ (6)$$

~~For a commercial B-III class HAWT with 92 m diameter rotor and 80 m hub height, at 10 m/s average velocity, the prescribed EOG and EVS for 1-year return period are presented at Figure 1. The time window in this figure starts and ends with the extreme event, which is 10.5s for 1-year return period.~~The β is a constant with value of 6.4 and the T is 12 s in the EWS. The peak factor of the EOG decreases with increasing size of the turbine or decreasing hub height, and vice versa for the ~~EVS~~EWS based on these equations.

Formatted Table

Formatted: Caption

Formatted: Font: Not Bold

Formatted Table

Formatted: Caption, Keep with next

Formatted Table

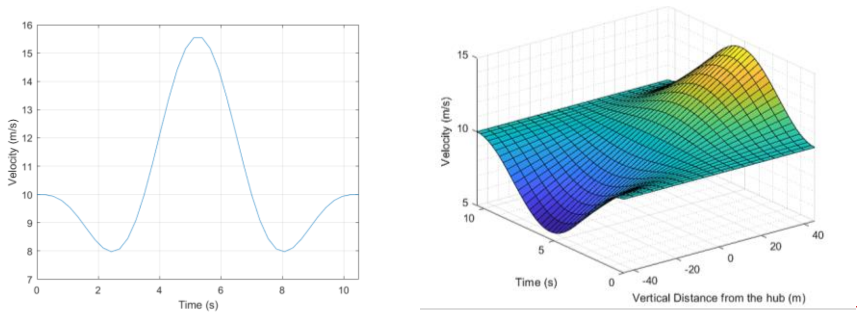

~~(a)~~ ~~(b)~~

~~**Figure 1: The extreme operational conditions with 1-year return period for a full scale HAWT class B-III with 92m diameter and hub height of 80m at 10 m/s uniform wind speed, (a) extreme operational gust, (b) extreme vertical shear on the rotor with hub height as reference**~~

Along with more common steady state experiments (Snel et al., 2007; Sørensen et al., 2002), developing transitory flow field experiments have attracted the interests of researchers during the past few decades (Lancelot et al., 2017; Ricci et al., 2017) to evaluate the various computational techniques or to directly investigate complex phenomena in different applications. To the authors' knowledge, in the wind energy field some efforts have been made to produce gusts using active grids (Petrović et al., 2019; Wester et al., 2018) and a chopper mechanism (Neunaber and Braud, 2020). Developing these unsteady flow fields basically comes down to the experiment targets and the available wind tunnel facilities. In this study, the generation of the EOG and the EWSs unsteady flow fields with ~~proper~~relevant scaling (customised for a 2.2 m scaled HAWT) using 60 individually controlled jet fans in the WindEEE dome are considered. This work presents a new numerical model of the WindEEE dome test chamber which can be used to predict fan settings for any custom steady or unsteady 2D flow fields before the physical experiment, and the capability of this facility to physically generate the gusts and shears similar to IEC standard during experiments. The focus of this paper is just on the time evolution of the simulated extreme conditions' flow fields which is a prologue for future experiments including an actual HAWT model.

The paper is organized in three sections beside the introduction and it is as follows. Section 2 details the development of the numerical model for the WindEEE test chamber which was used to obtain the fan setups to use in physical simulation of the gusts. This section also provides a length and time scaling of the gust which based on that the target gusts for experimental campaign are introduced. Section 3 presents the results from velocity measurements at the test section in two parts, firstly the steady shears to assess the accuracy of the developed numerical model to simulate the shear layers and secondly the final transient simulated gusts and their comparison with IEC standard. Section 4 provides some conclusions.

2. Methodology

2.1. WindEEE Dome

The physical experiments were conducted in the WindEEE Dome at Western University, Canada. This is a versatile facility that can be run at different modes for creating various non-stationary wind systems (Hangan et al., 2017). It has an inner test chamber with a 25 m diameter hexagonal footprint and 3.8 m height. ~~The dome inner shell and the flow path in the closed-circuit 2D flow mode (e.g. ABL, shear flows and etc) are rendered in Figure 2a.~~ ~~The test chamber is in turn surrounded by an outer shell.~~ It has a total 106 fans, including 60 fans installed on one wall and 40 fans over the other five peripheral walls. There are also 6 larger fans in a plenum above the test chamber which are mostly used for generating 3D flows like tornados and downbursts. The test chamber is in turn surrounded by an outer shell. ~~The side view schematic~~The dome inner shell/test chamber along with outline of the ~~dome is shown at~~ outer shell with the flow path in the closed-circuit 2D flow mode (e.g. ABL, shear flows and etc) are presented in Figure 1~~b to describe the flow recirculation path in the closed-circuit~~ a. In 2D flow mode~~. In this mode~~, the louvers at the top and peripheral sides of the test ~~section~~chamber are closed and the flow ~~energizes~~is energized only by the 60 fans, then it reaches to the test section (center of the test chamber) and then exits the test chamber through the mesh of the wall at the opposite end, then recirculating over the top while passing through the heat exchangers, and finally back to the 60 fans' inlet. Each fan is 0.8 m in diameter with 30 kW nominal maximum power. In order to reach higher velocities and better flow uniformity characteristics at the center of the test chamber, a two-dimensional contraction can be setup to streamline the flow as shown in Figure 1~~c~~b.

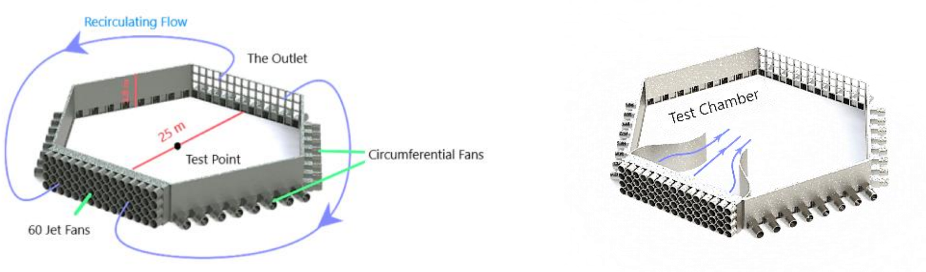

Inserted Cells

Formatted Table

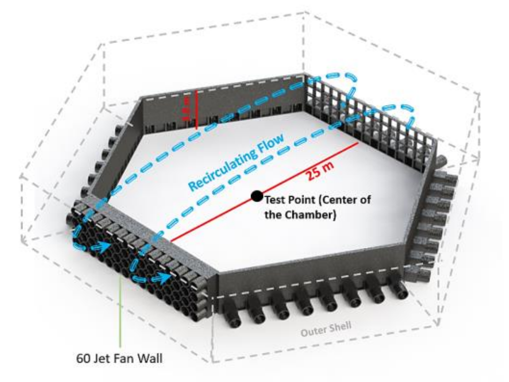

(a)

(b)

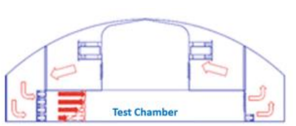

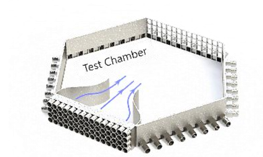

~~(b)~~ ~~(c)~~

Figure 1. A brief geometry of the WindEEE ~~hexagonal~~ dome, (a) the test chamber~~, (a) render of test chamber and~~ with outline of the outer shell along with the flow path~~, (b) side view schematic of the WindEEE dome with flow path~~ in closed-circuit ~~straight~~2D flow mode, (~~c) render of~~b) the test chamber with contraction walls

Formatted Table

The power set-points of the 60 fans can be adjusted by the software as fast as 2Hz. However, this does not imply the fans themselves can throttle from 0% to 100% power at 2 Hz (due to rotational inertia of the fans' rotors and electrical current filtering it takes ~3 s for the fans to adjust).

Another feature are the fans with adjustable inlet guide vanes which can regulate the amount of ~~mass~~ flow rate through the fans. These vanes can be adjusted uniformly from 0% open (close) to 100% open (Figure 2). They can also be adjusted dynamically by setting an actuation frequency, duty cycle and an initial position. The actuation frequency specifies the time between two cycles, while the duty cycle specifies the duration of an individual cycle specified as a percentage of the time between two successive cycles. All these features allow the generation ~~of repeatable and~~ customisable dynamic flows.

(a) (b)

Figure 2. The adjustable vanes at the inlets of the 60 fans wall, (a) 100% open vanes, (b) 70% open vanes

2.2. Numerical Flow Analysis Setup and Tuning/Validation

In order to have a better understanding of the flow field in the test chamber, a numerical model for the test chamber was created using the commercial Star-CCM+ CFD software, which helped to predict the fan power setups for different scenarios prior running the experiments.

For this purpose, four simplified symmetrical domains of the test chamber were generated to save considerable CPU time as listed at Table 1. As this table outlines, the domains V and V-c were used for simulating EOG, EVS and ABL flows; domains H and H-c were used for simulating EHS.

Formatted: MDPI_3.1_text

Table 1: The symmetrical domains of the test chamber used for simulating different cases

Picture of the Domain	Application	Domain ID
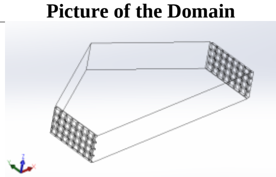	Simulating ABLs and EVS & EOG and tuning the boundary conditions parameters	V
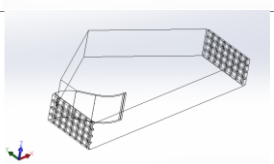	Simulating ABLs and EVS & EOG with contraction walls and tuning the boundary conditions parameters	V-c

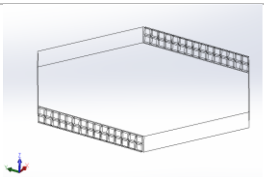	Simulating EHS	H
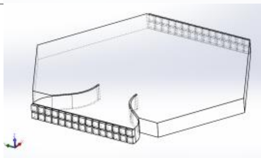	Simulating EHS with contraction walls	H-c

In order to discretize the domains, three mesh setups (M1, M2 and M3) were considered for the polyhedral automated mesh function, built-in Star-CCM+ software. The general details for the generated grids are presented in Table 2. For all the cases, 5 prism layers with a total thickness of 0.~~05m~~05 m and with stretching of 30 % at the solid walls with minimum of 4 elements in the gaps were used; ~~other parameters~~the surface curvature and surface growth rate were left ~~as~~at their default values~~.~~ (6 degree and 20% respectively) with no specified mesh density in the domains. In addition, in domains with contraction walls a custom control refinement on the ~~surface~~surfaces of the contraction ~~wall~~walls was used to create elements half of the general base size. The fans were modelled as squares with individual velocity inlet boundary conditions~~ per fan~~. The outflow grid on the opposite wall was treated as uniform pressure outlet. All other surfaces were treated as no-slip walls. Due to broad range of the Reynolds number across the domain, controlling the wall y+ was challenging. Therefore, for modelling the Reynolds stresses in the RANS equations, two-layer K-epsilon (k-ε) turbulence model was chosen.

The next step was to calibrate the boundary condition parameters based on the previous experiment data that were available for scaled ESDU ABL profiles both with and without contraction walls (Hangan et al., 2016). The simulated fan powers were then adjusted to reach the desired average velocity profiles at the test section to match the existing experimental data. The M1 setup at domain V and V-c were used for preliminary tuning of the input values at the inlets and the outlet boundary condition parameters in order to get the best match with the available data at the test section. The best results corresponded to an inlet turbulence intensity of 8% with length scale of 0.2 m and the outlet boundary set as a pressure outlet with uniform zero-gauge pressure, 1% turbulence intensity and 0.05m length scale. Working at full power, the fans can generate 13 and 31 m/s of uniform wind velocity at the test section without and with contracting walls respectively. ~~In~~At the end the simulation results showed that the full fan powers corresponded to a 16.5 m/s inlet boundary velocity. The fan power set-points were then simplified as a linear interpolation between 0 and 16.5 m/s for the velocity inlets.

Table 2: Detail of grid sizes for each domain

Grid name tag	M1	M2	M3
Number of Cells for Domain V (Million)	1.41	2.53	5.52
Number of Cells for Domain V-c (Million)	2.37	3.72	6.75
Number of Cells for Domain H (Million)	N/A	1.93	N/A
Number of Cells for Domain H-c (Million)	N/A	3.00	N/A
Base size (m)	0.1	0.08	0.06

The mesh independency check was defined by the incrementally refined grids M1 to M3 using the velocity profiles at the test section for the ABL profiles which have different fan power set points for each row (Figure 3). For low speed setup (without contraction) they were at 50, 70, 70 and 50% from bottom row to top (Figure 3a); ~~for~~in the setup with contractions, the fans are at 50, 65, 75 and 75% (Figure 3b~~);~~). The velocity profiles from the CFD results ~~was~~were defined by a vertical probe line ~~at~~passing through the center of the test chamber with 40 elements over the entire height of the chamber.

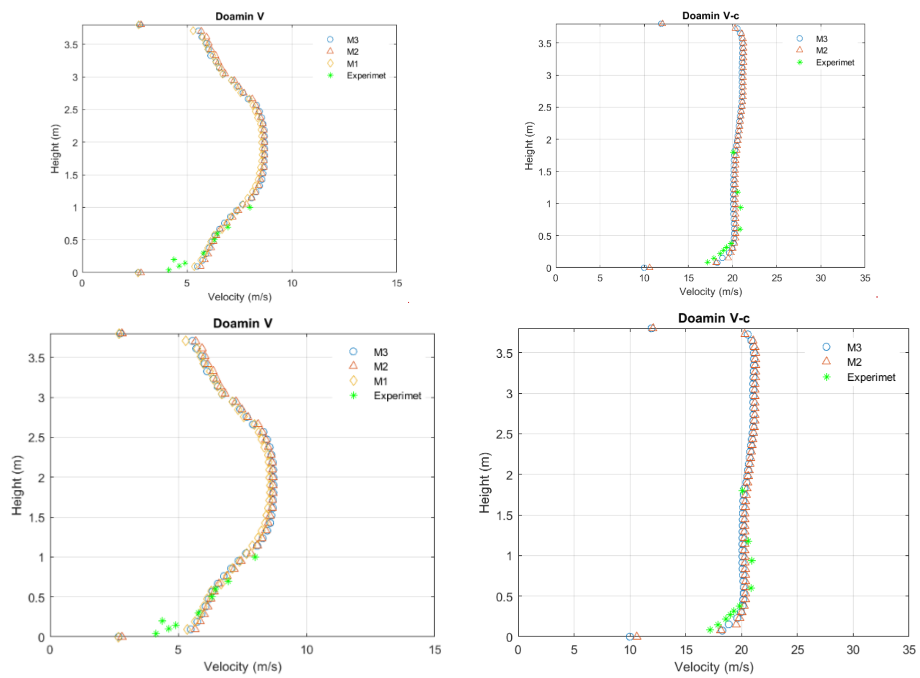

(a) (b)

Figure 3. The mean ABL velocity profiles at the test section for different mesh setups comparing with the experimental data (Hangan et al., 2016)**, (a) low speed (without contraction) and (b) high speed (with contraction) mean velocity vertical profiles**

~~According to~~ Figure 4a &b ~~showing~~show the relative errors between velocities at each height~~,~~; the largest disconformities between different mesh setups occur close to the wall~~,~~ which for this research is not the most important region. The more critical region for the present experiments is at the middle heights where the wind turbine rotor will be located. That being said, even the M1 setup has an acceptable range of error (~1%) at mid-height. However, the M2 mesh setup was chosen as the best compromise of computation speed and accuracy.

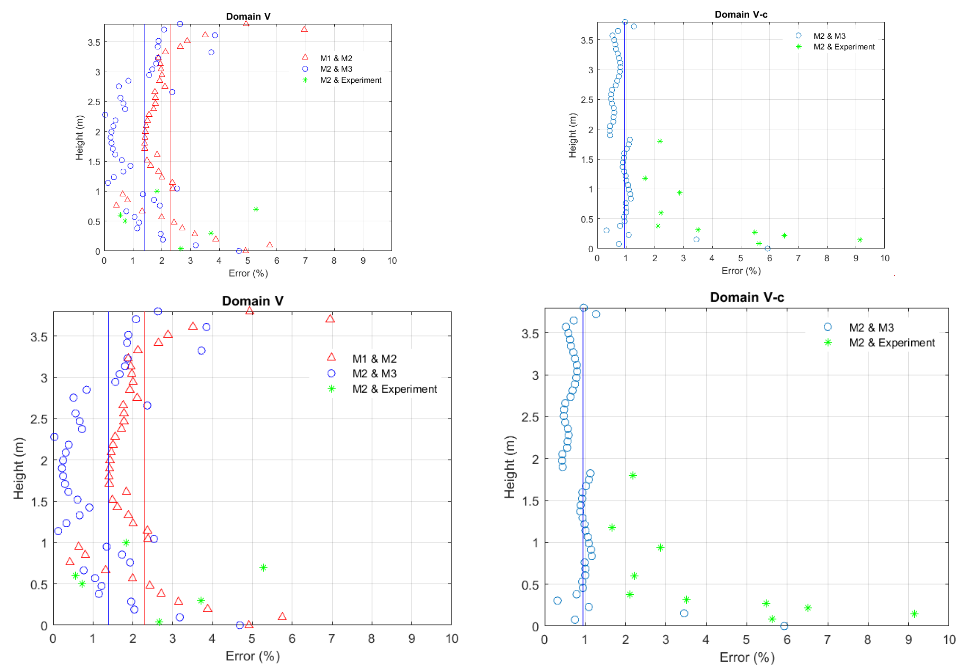

(a) (b)

Figure 4. The relative errors for (a) low speed velocities and (b) high speed velocities, the solid lines are the mean value for the errors over the whole height

The discrepancy between the CFD simulation (M2) and the experimental data also increases close to the wall. This error is rooted in uncertainty of the implemented turbulence model and relative course mesh size close to the wall in the numerical model. Nevertheless, they are in an acceptable range of engineering applications (under 10% of relative error). A picture of discretized domain V-c with the M2 grid is shown ~~at~~in Figure 5.

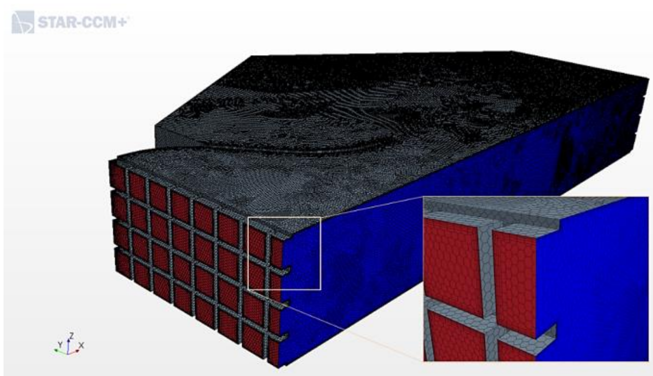

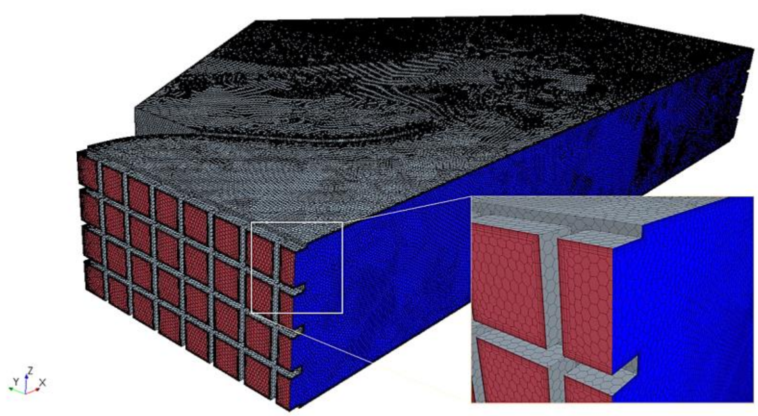

Figure 5. The M2 grid for the V-c domain

As described, this numerical model has been developed based on a set of steady ABL experimental data. The first application of it was to generate a calibration table that related the steady fan power set-points to the mean velocity magnitudes and profiles at the test section. This table was used to predict the fans' powers in generating the EOG. For simulating the EWSs, only the peak stages of these extreme events were considered for modelling, again in steady condition in order to obtain the fan setups at the peak of the corresponding wind shear event (see 3.1). These numerical simulations neglect the closed loop flow recirculation dynamics in the dome. Nevertheless, it produces a reasonable prediction of the fan setups for a specific flow field in a reasonable amount of time.

2.3. Experimental setup for velocity measurements

The velocity measurements were obtained with seven cobra probes. Each probe has 4 pressure tabs at the head (0.5mm each) and is able to measure three velocity components with measuring range from 2 to 45 m/s with $\pm$0.5 m/s accuracy (TFI Ltd., 2011). In this study, the average wind velocity was 5 m/s; therefore, all of the wind measurements have ~ 10% accuracy in average.

Two different setups for velocity measurements were used:; vertical and horizontal arrangements (Figure 6). The seven cables from all the cobra probes were connected to an interface box. The output cable from this box then was connected to a laptop via an analog to digital converter card. The sampling duration was 60 s with sampling frequency of 2000 Hz for each measurement run. In each extreme event multiple actuation times for modulating either the fan powers or the IGVs were considered; this study presents the best results compared to the target extreme events from an individual test run.

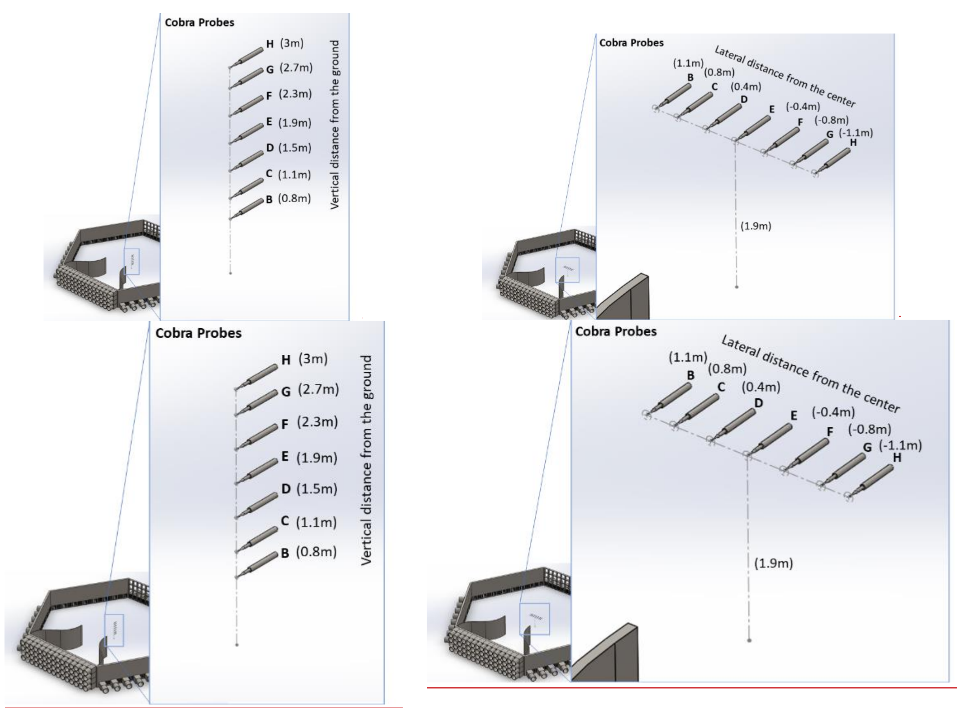

(a)

(b)

(c)

Figure 6. The arrangement of cobra probes based on the dimension of a 2.2m diameter HAWT for (a) vertical and (b) horizontal measurements at the center of the test section, (c) Setting up the 7 cobra probes in a horizontal arrangement at the test section

The ~~location~~locations of the probes ~~was~~were chosen based on the dimension of the available wind turbine in the facility. This turbine has a 2.2 m diameter with adjustable hub height, chosen as 1.9 m (Refan and Hangan, 2012). This entire paper is dedicated just to the development of the flow field. Investigation the effect of these unsteady wind conditions on the turbine is left for future work.

2.4. Gust length and time scaling

The time ~~duration of the gust (T), as mentioned earlier, is 10.5 s for a 1-year and 14 s for a 50-year return period in the IEC standard. The gust duration corresponds~~durations of the extreme events (T), as mentioned earlier, are 10.5 s for EOG and 12 s for EWS (IEC, 2005). Subsequently, the gust durations correspond to 3 to 4 complete rotor revolutions periods for full-scale turbines (which usually have angular speed of 15-18 RPM in 10 m/s average wind speed~~), which for the~~). For a scaled wind turbine in the wind tunnel ~~would be~~4 rotor revolutions happen on the order of a second at the nominal operating condition. This gust time scale would be impossible to simulate at WindEEE facility given the physical limitations of the hardware.

Therefore, we assume that the time scale of the gust is equal to propagation time of 4 loops of a blade tip vortex downstream in the wake. We can then calculate the propagation length and time of these vortex loops based on the definition of the Tip Speed Ratio (TSR: $\frac{blade\ tip\ speed}{free\ stream\ speed}$~~) and~~); assuming a uniform wake we have:

$$\Omega = \frac{\lambda U_{hub}}{R}[rad/s],$$

Formatted Table

$$\Omega' = \frac{\lambda U_{hub}}{R}\times\frac{1}{2\pi}[rev/s], \quad \text{~~(5)~~ (7)}$$

$$U_{hub}\times\frac{1}{\Omega'} = \frac{2\pi R}{\lambda}\left[\frac{m}{rev}\right],$$

where Ω is the angular velocity in radiant per second and Ω' is in revolution per second, λ is TSR and R is the radius of the rotor~~. Which~~; with some rearrangement the last part in equation (7) can be rewritten as follow:

Formatted: Caption, Keep with next

$$\frac{L'}{D} = \frac{T'U_{hub}}{D} = \frac{\pi}{\lambda}, \quad \text{~~(6)~~ (8)}$$

Formatted Table

the L' and T' are the length and time duration for propagation of one vortex loop in the wake. Based on the ~~Eq. (6)~~equation (8) and our assumption, an appropriate gust time and length can be calculated from:

$$\frac{\boldsymbol{L_s}}{D} = \frac{\boldsymbol{T_s}U_{hub}}{D} = 4\frac{\pi}{\lambda}\cancel{,} \quad \text{~~(7)~~ (9)}$$

Formatted Table

Accordingly, the scaled time duration (T_s) is function of TSR, free stream velocity and the diameter of the rotor. The scaled length (L_s) is function of TSR and diameter of the rotor (Figure 7).

If the scaled turbine works at the same TSR and free stream velocity as the full-scale commercial HAWT, the time and length scale would be equal to their geometrical scale (i.e. the ratio of diameters).

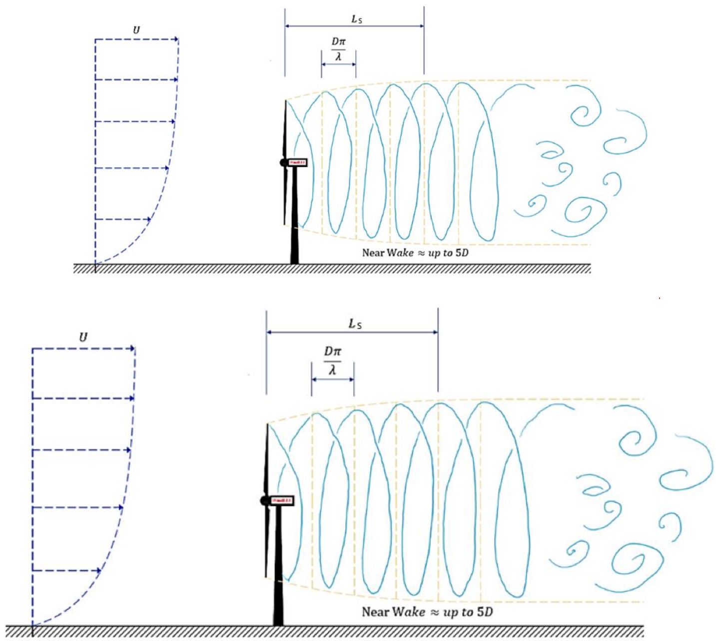

Figure 7. Visual representation of the length and the time scale ~~proper for~~relevant to the extreme conditions with assuming a symmetric wake

The flow behaviour in the near wake region is directly correlated to the overall performance of a HAWT. Matching the time duration of the extreme condition to the propagation of 4 vortex loops in the wake should be a reasonable comparison to the full scale in terms of variation of power and loads on the wind turbine.

For a commercial B-III class HAWT with 92 m diameter rotor and 80 m hub height, at 10 m/s average velocity, the prescribed EOG and EVS are presented in Figure 8a & b. The time windows in these figures start and end with the extreme events.

The physical experiments showed that the fastest possible gust events with the required peak factor were ~~at time scales of~~around 5 seconds due to the hardware limitation. Therefore, ~~based on our assumption, this requires~~to match the extreme event period to the suggested scaling assumptions, the 2.~~2m~~2 m scaled wind turbine ~~to~~should work in ~~5m~~5 m/s free stream velocity with operating TSR of 1.1, then it would take 5 seconds for the four complete loops of the tip vortexes generated by a specific blade to propagate in the wake. Accordingly, in all of the simulations and experiments the hub height velocity was kept at 5 m/s~~ to increase the time scales. In this setup, the ratio of the length and time scale become 5.23 and 2.61 respectively.~~

~~The Reynolds number calculated from the relative velocity and chord size at 70% span of the blade for full scale turbine at the nominal wind speed and TSR (10 m/s and 8 respectively) is $\sim 7.5 \times 10^6$ and for the scaled turbine at the~~ .~~our lab condition is $\sim 32.5 \times 10^3$ which gives the ratio of ~ 230. This mismatch can be improved by being capable of running the experiment at higher wind velocities and TSRs.~~

~~All of the simulations and experiments were tailored for the available scaled wind turbine.~~ Assuming a similar B-III class for the scaled HAWT with the hub height of ~~$\sim$10~~2 m ~~for~~, the ~~2.2 m rotor, the~~scaled extreme condition profiles ~~look identical to the full-scale ones (the same peak factor but different gust time) at 5 m/s average hub-height velocity considering 1-year return period, as it is~~are shown in ~~Figure 9.~~

~~Accordingly, for the~~Figure 8c & d; in the scaled EOG ~~the~~ velocity should uniformly rise from 5 to ~~9.5~~ $\sim$7.8 and then back to 5 m/s in 5 seconds with $\sim$1~~.5~~ m/s ~~drop~~drops before and after the main peak relative to the average free stream velocity (~~Figure 9a).~~Figure 8c). However, in the experiments the gusts have been simplified by not including the velocity ~~dips~~drops (the red dashed~~-~~ line in ~~Figure 9a).~~Figure 8c). This simplification stretches the actual rising and falling time from $\sim$ 2.5 to 5 s. ~~This~~Yet, this is the compromise that was made due to the hardware limitations ~~and for having a consistent total gust time duration with~~. Hence, in this study, the target EOG has the same falling and rising time period as the scaled EWSs. The pre-post dips in the standard EOG reflect field data wherein gusts are preceded by lulls; however for the purpose of investigating peak loading during gust events, for a machine nominally operating at the mean wind speed and assumed not responding much during the lull period, it is the velocity excursion above average wind speed that is important to capture. Future apparatus design and fan control may enable execution of ~~per~~pre-post lulls in ~~future~~prospective experiments.

~~For~~In the scaled EVS the uniform velocity field transitions to a highly sheared flow ($\sim$7 m/s velocity shear ~~in~~over 2.2 m distance) and then back to a uniform field, again in 5 seconds (~~Figure 9b). For the full scale the same amount of velocity difference happens over 92 m with different time scale.~~Figure 8d).

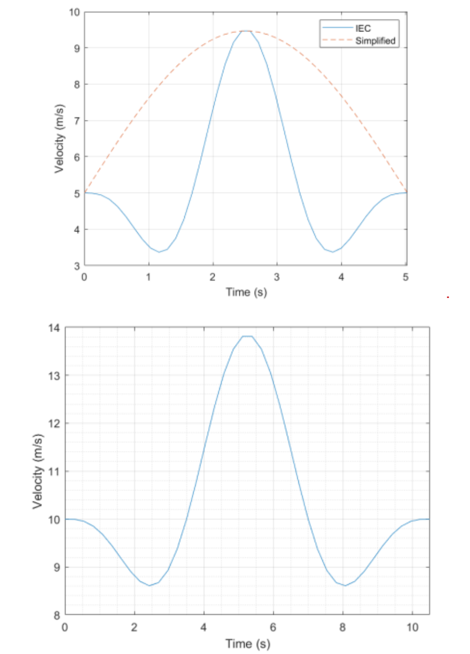

(a)

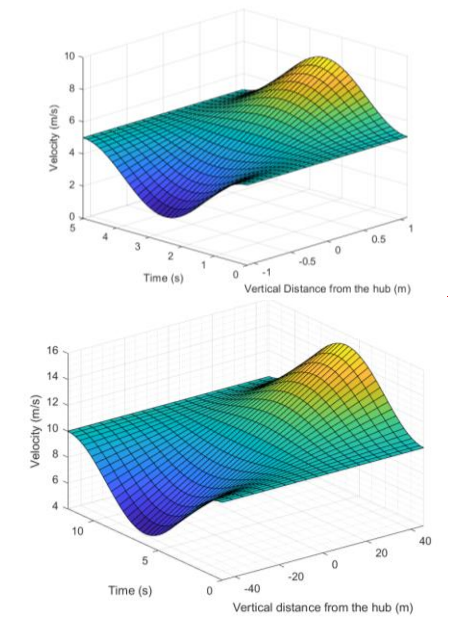

(b)

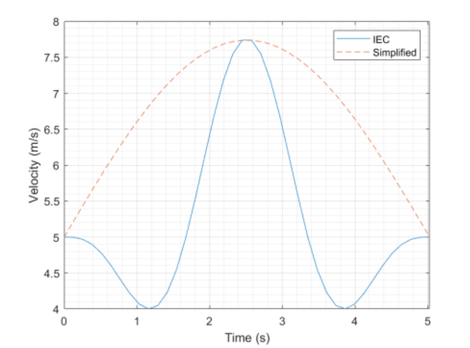

(c)

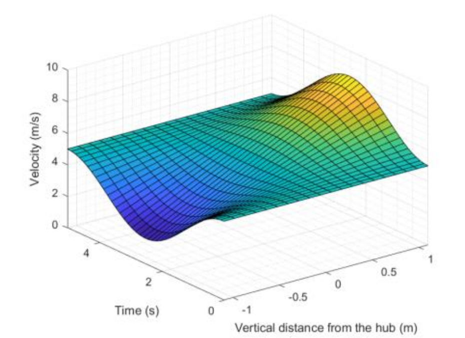

(d)

Formatted Table

Figure 8~~.~~: The ~~target~~ extreme operational conditions for ~~simulations~~a full scale HAWT class B-III with 92 m diameter and ~~experiments based on~~hub height of 80m at 10 m/s uniform wind speed compared with the scaled ~~wind~~ conditions for a B-III turbine with 2.2 m diameter and ~~capability of the fans, identical to prescribed~~2 m hub height at 5 m/s average wind speed (a) full scale extreme ~~condition for the~~operational gust, (b) full~~-~~ scale ~~wind turbine just with different time scale, (a)~~extreme vertical shear, (c) scaled extreme operating gust, the solid blue line is for IEC and the simplified gust that actually was ~~produced~~targeted is in red dashed ~~-~~line, (~~b)~~d) scaled extreme vertical shear

Formatted Table

In these settings, the length and time scale ratios are 5.2 and 2.4 respectively. The Reynolds number based on the relative velocity and chord size at the 70% blade span for full scale turbine at the nominal wind speed and TSR (10 m/s and 8 respectively) is $\sim 7.5 \times 10^6$ and for the scaled turbine at our lab condition is $\sim 32.5 \times 10^3$ which gives the ratio of ~ 230.

3. Results and discussion

3.1. Steady wind shear

In this section the simulation cases are all steady and just for the peak ~~stage~~stages which is the instantaneous point in time that maximum shear occurs, as a preliminary investigation to unsteady experiment runs that are examined in the next sub-section. Using the tuned numerical model ~~setups~~, the V-c and H-c domains were used to simulate the desired vertical and horizontal sheared flows by ~~manipulating~~modulating the input velocity for the different rows and columns of the fans. The target was to match ~~as closely as possible~~ the velocity profile as similar as possible to the IEC standard for the scaled HAWT, corresponding to ~7 m/s shear while keeping the velocity at the rotor centerline 5 m/s. Figure 9 shows the fan setups using CFD for creating the desired shears which could be achieved by using only the 5 fan columns at the middle. For creating negative vertical shear, the setup presented in Figure 9a was inverted.

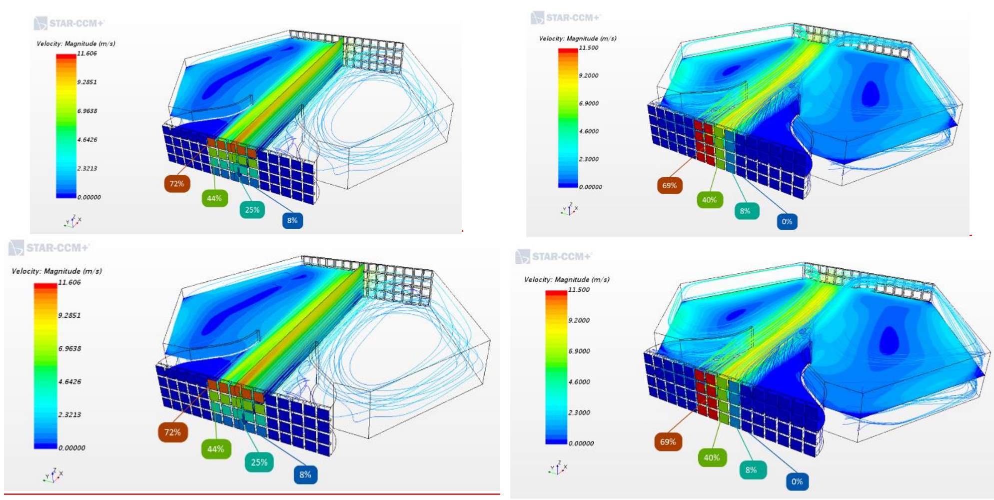

(a) (b)

Figure 9. Fan setups for peak stages of extreme (a) vertical and (b) horizontal shears, prescribed for the scaled HAWT identical to full scale condition, the power set-points for each row and columns ~~is~~are included (just the 5 columns at the middle are working)

Using the fan setups shown in Figure 9 the physical ~~experiment was~~experiments were carried out and velocity measurements made using the ~~Cobra~~cobra probes. Figure 10~~ shows~~a, b & c show the average velocity at each probe including the range of velocity ~~deviation~~fluctuations (standard deviation) compared with average velocity profile from the CFD (dashed-line) and the prescribed shear by IEC standard~~. These~~ (yellow solid-line) for the EVS, EHS and negative EVS respectively. The high ~~amount of~~ velocity fluctuations relative to the mean velocity in experiments are due to the strong vortexes that form in these highly sheared flows ~~that~~which increase the momentum mixing at different heights. The amount of shear that was prescribed (~7 m/s velocity difference) is being successfully created in the tunnel for the positive vertical shear case (Figure 10a). However, for the horizontal and negative vertical cases (Figure 10b & c) there are larger shears than desired, resulting in a ~10 m/s velocity difference. From Figure 10a & c it is clear that the lower fans work more efficiently than the upper fans~~;~~ (i.e. with the same value of the power set-~~point~~points, the lower fans generate higher velocities~~.~~). The largest disconformity exists in the horizontal shear case (Figure 10b).

The relative ~~difference~~discrepancy between the mean ~~velocities from~~velocity fields of these three ~~steady~~ experimental ~~data with~~steady shears and the IEC ~~standard is~~are presented ~~at~~in Figure 10d. Accordingly, the average amount of disconformities over all of the probes are 41, 27 and 9 % for the horizontal, the negative vertical and the vertical steady shears respectively~~ which can be adjusted in future~~. Basically, this comparison revealed the capability of the developed numerical model to predict the fan setups for simulating the EWS. As was explained in section 2.2, the numerical model is tuned just based on previously tested ABL flows while assuming similar efficiencies for all the fans, neglecting the flow recirculation in the outer shell and simplifying WindEEE test chamber geometry. The fan power values in all the test cases (steady and unsteady) are directly taken from the steady numerical model prediction results. In future, further field adjustments are required to generate a flow field as similar as possible to the IEC prescription.

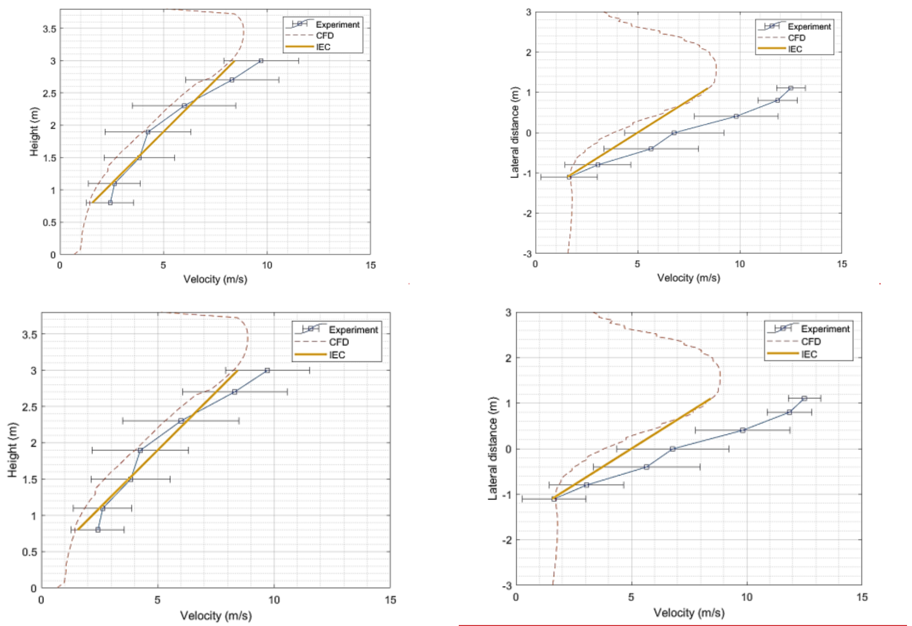

(a) (b)

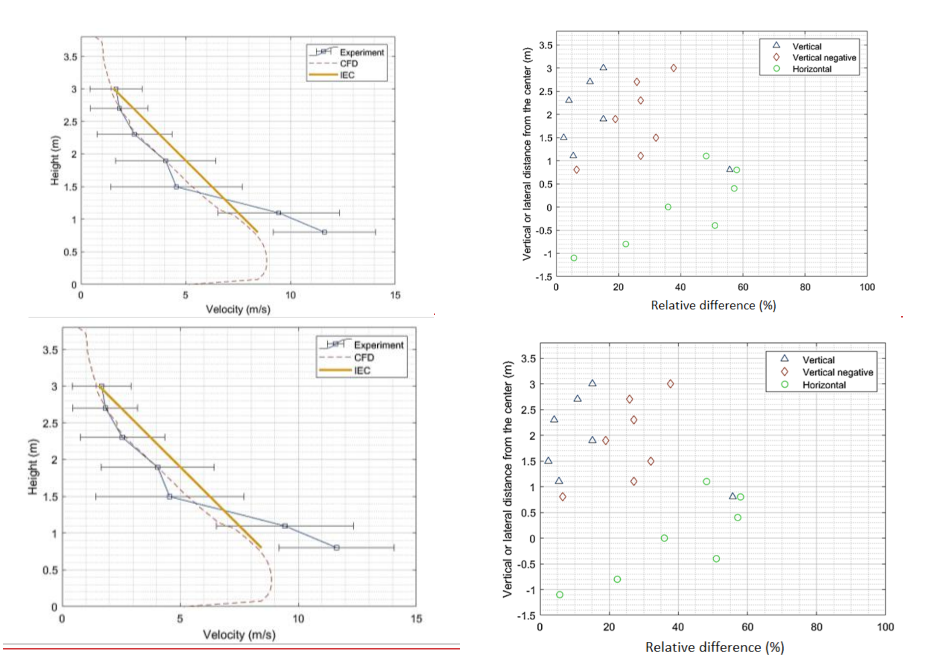

(c) (d)

Figure 10. CFD predictions vs experiment data for steady (a) vertical shear, (b) horizontal shear and (c) negative vertical shear, (d) the relative disconformity between the three steady shear experiments and IEC standard

3.2. Unsteady experiments

For the shear cases just the five columns of the fans in the middle were working (only 20 out of 60 fans were operated). ~~For the nominally~~The uniform ~~inflow condition, at the beginning~~flow field before and ~~the end of~~after the shear events, ~~they were all set~~ generated by setting these 20 fans at 39% power. The best results in terms of the event duration, were captured when the extreme condition ~~setup (the setup at Figure 10) was set to~~ setups were set for 1.6 s in the actuator software~~.~~ (i.e. the fan powers uniformly stayed at 39% and then switched to the setup in Figure 9 for just 1.6 seconds then back to the 39% uniform). The uniform gusts were generated in two ways. The first was again by changing the power set-points of all the ~~all~~ 60 fans together. According to the results from the CFD simulations (Domain V-c), in order to achieve the prescribed EOG, the fan power set-points should uniformly go from 17% to 30% ~~(correspond to 5 and 9.3 m/s wind at test section)~~ and back to the 17% power. For the uniform gust, the best result again was obtained with switching fans ~~on~~to 30% for 1.6 s which resulted in ∼5 s uniform gust with desired peak factor. The second way of generating a uniform gust was using the IGVs while keeping fan power set-points constant at 30%. In this run, the actuation frequency of the IGVs was set at 0.05 Hz with a duty cycle of 8%, initial position of 10% open with cycling to 100% open (see section 2.1 for IGV setting definitions). In addition, ~~for~~in each uniform gust case, to obtain a better understanding of the uniformity of the flow field, two measurement runs were conducted ~~in order to measure the velocity field with~~ using both vertical and horizontal layouts of the cobra probes (~~layout~~layouts in Figure 6~~) in order to investigate the uniformity of the inflow. All~~). For processing the data all of the velocity time histories were filtered using a moving average with an averaging window of 0.2 s based on the criteria described at (Chowdhury et al., 2018).

3D pictures of the filtered turbulent wind fields for the EVS, EHS, negative EVS, EOG cases generated with changing fan powers (vertical & horizontal measurements), and the EOG generated using the IGVs (vertical & horizontal measurements) are presented in Figure 11a, b, c, d & e, f & g respectively. ~~From~~The average amount of variation in reading the velocity values due to the filtration is $\pm$0.16 m/s for the EWS cases; $\pm$0.11 m/s for the EOG using the fan powers and $\pm$0.41 m/s for the EOG using the IGVs. In Figure 11a & c when the 20 fans ~~in the~~at middle are operating, it is again evident that the fans ~~in~~at the top row do not work as ~~efficiently~~efficient as the other fans~~,~~; they could have less stable air supply than the lower rows which ~~could~~should be due to the tight direction change of the recirculating flow ~~in the recirculation process~~ from the top. Figure 11d & f show ~~velocities~~velocity fields when all 60 the fans are operating with the contraction walls to help ~~unify~~unifying the flow field. Figure 11b, e & g show that all of the flow fields are horizontally uniform. The data from the EOG generation with IGVs (which work in a cyclic manner) in Figure 11f & g shows the background velocity fluctuations are high relative to the EOG generation by manipulating the fans' powers ~~at~~in Figure 11d & e.

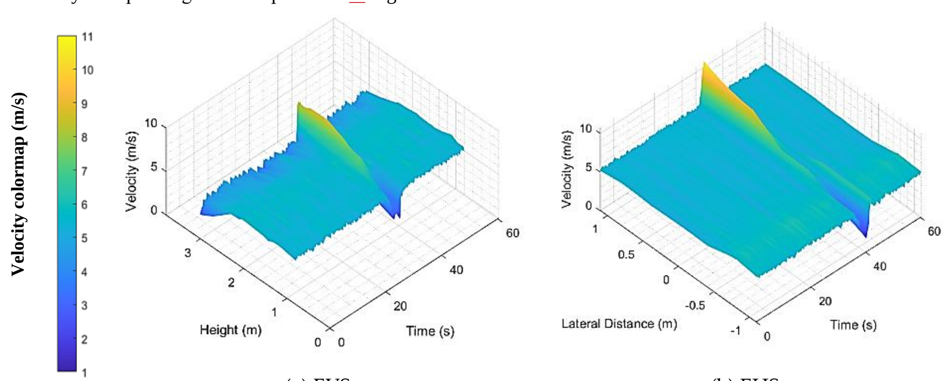

(a) EVS

(b) EHS

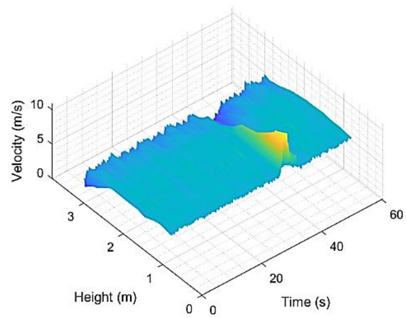

(c) negative EVS

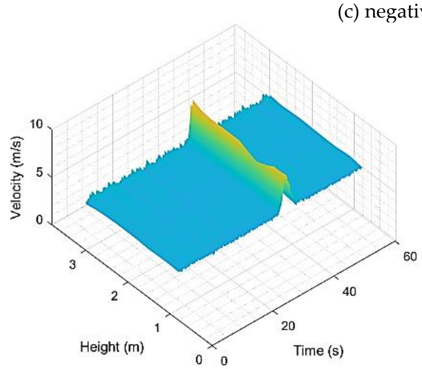

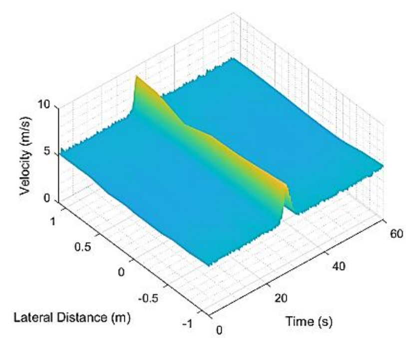

(d) EOG generated with changing fan powers, vertical measurements

(e) EOG generated with changing fan powers, horizontal measurements

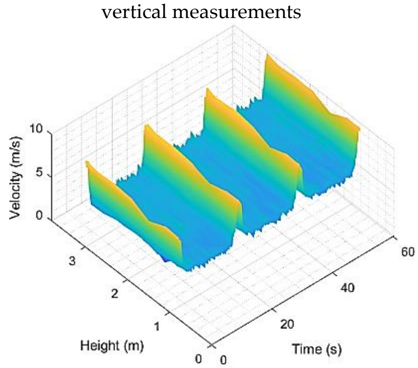

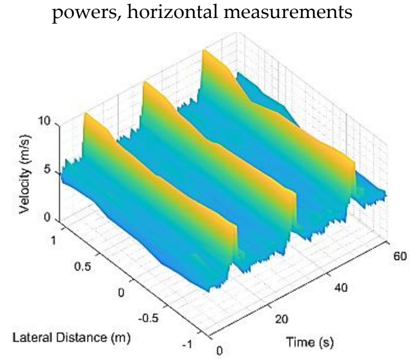

(f) EOG generated with IGVs, vertical measurements

(g) EOG generated with IGVs, horizontal measurements

Figure 11. 3D pictures of the complete time history of the phased averaged (with 0.2 s averaging window) turbulent velocity field

In order to have a better comparison of ~~the generated extreme~~these unsteady cases with ~~what~~ the ~~standard prescribes~~IEC, the velocity time history extracted from the cobra probes B to H (with the layout showed in Figure 6~~, as well as~~) in blue solid-lines along with the standard specifications in orange solid-lines are plotted ~~as solid blue and orange lines respectively in~~ in Figure 12 ~~in~~at the left columns (~~the~~ cases are in the same order as Figure 11). The right ~~column contains~~columns contain the relative instantaneous discrepancy of the velocity relative to the IEC prescribed velocity, normalized by the average velocity ($\sim 5\ m/s$).

Based on data for the shear cases, at the peak stages the amount of desired shear is successfully being generated. However, due to the difference in velocities, there is a time lag between the peaks' locations at the top to bottom heights of the EVS cases, and left to right in the EHS cases (Figure 12a, b and c).

As ~~mentioned earlier~~previously discussed, when just the 20 fans in the middle ~~of the wall~~ are working the lower efficiency of the top row of the fans is more noticeable ~~due to the tight angle of flow recirculation~~ at probe H in Figure 12a & c~~.~~; the velocity time history at this height and condition has more fluctuations compare to the other probes. Probe H in Figure 12d & f shows in better detail that using all the 60 fans and the contraction walls helps ~~homogenize~~homogenizing the flow field~~.~~ ~~However~~ close to the ceiling (i.e. similar velocity magnitudes and fluctuations in all the time histories across the probes). Yet, in the gust peak ~~the problem still shows itself~~when the flow is highly dynamic, the insufficiency of the air supply for the top row is noticeable as ~~velocity intermittency as~~ the probe H in Figure 12d demonstrates~~.~~ (the sudden velocity drop while the velocity in other probes consistently increasing). Similar velocity ~~intermittencies~~instabilities have been ~~noticed~~observed at the same height in other experiment runs when rapid fan power changes ~~are applied. However, the desired~~were applied. Figure 12d & e in detail present the flow field of the EOG generated by changing the whole 60 fans' powers. In the discrepancy time histories, there are double hump shape profiles mostly due to the two sequential velocity drops before and after the main velocity hike in the standard. Even though the peak factor ~~has been generated~~is being captured the gust profile is not symmetric as the standard suggests; the second humps in the discrepancy time histories consistently have higher magnitudes. This could be due to the fact that the fans do not decelerate as fast as they can accelerate (the gust falling time is not as fast as its rising time). Active fan braking might be explored in future work to accelerate the falling gusts, instead of relying on inertia/friction.

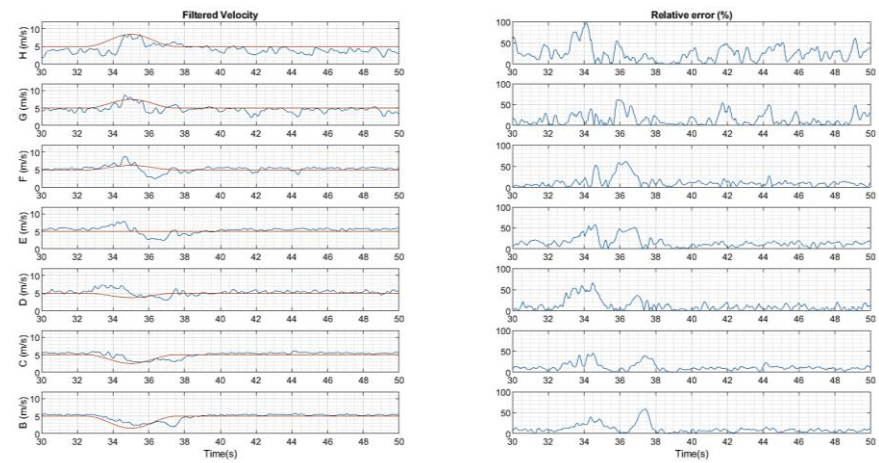
Filtered Velocity
Relative error (%)
H (m/s)
G (m/s)
F (m/s)
E (m/s)
D (m/s)
C (m/s)
B (m/s)
Time(s)

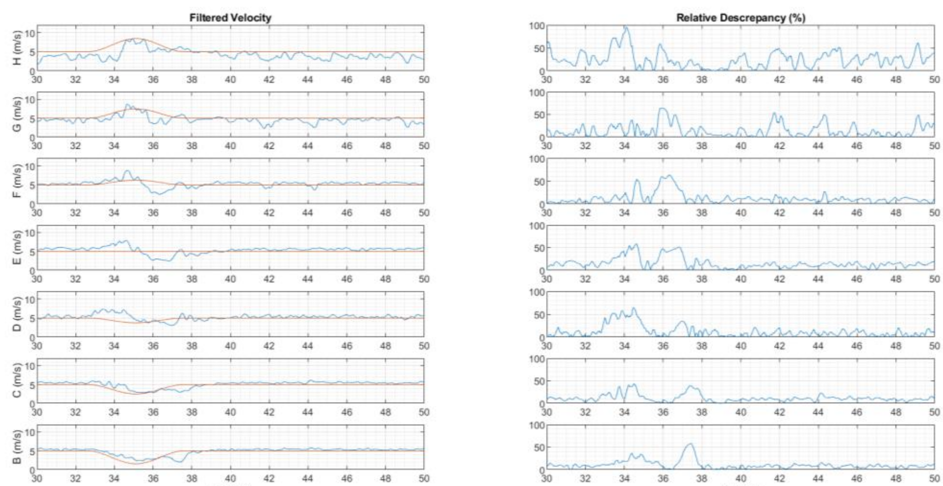
Filtered Velocity
Relative Descrepancy (%)
H (m/s)
G (m/s)
F (m/s)
E (m/s)
D (m/s)
C (m/s)
B (m/s)
Time(s)

(a) EVS

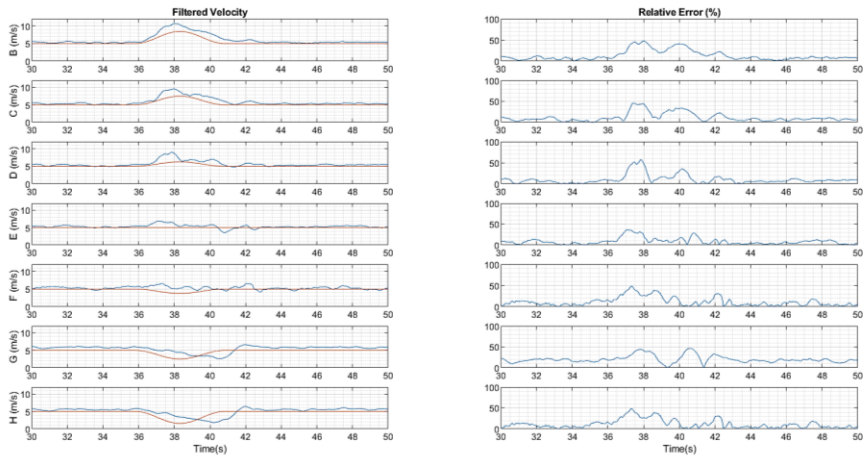
Filtered Velocity
B (m/s)
C (m/s)
D (m/s)
E (m/s)
F (m/s)
G (m/s)
H (m/s)
Time(s)
Relative Error (%)
Time(s)

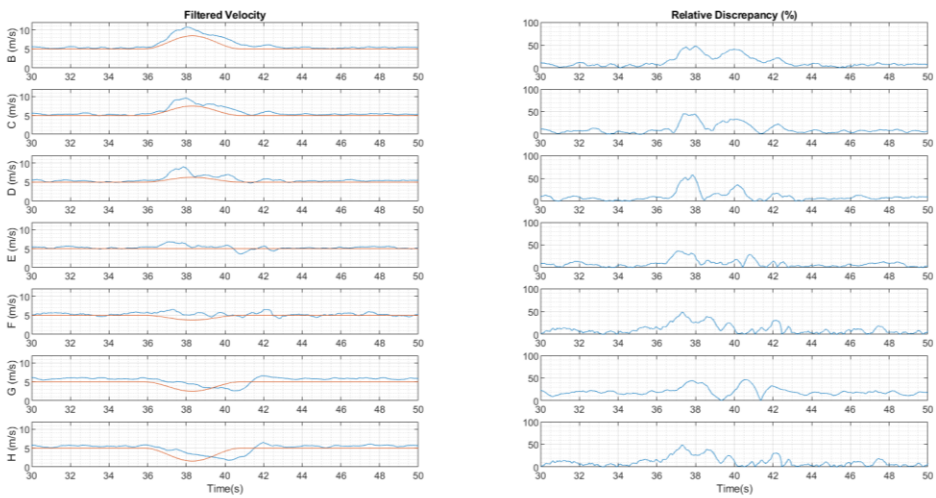
Filtered Velocity
B (m/s)
C (m/s)
D (m/s)
E (m/s)
F (m/s)
G (m/s)
H (m/s)
Time(s)
Relative Discrepancy (%)
Time(s)

(b) EHS

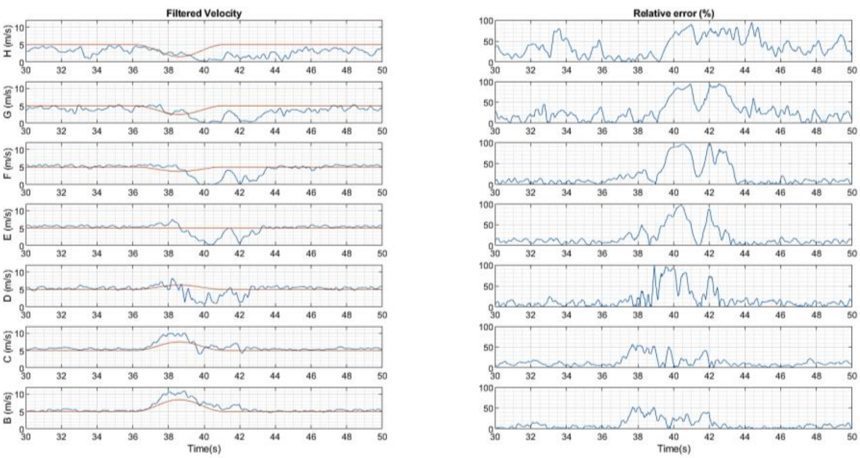

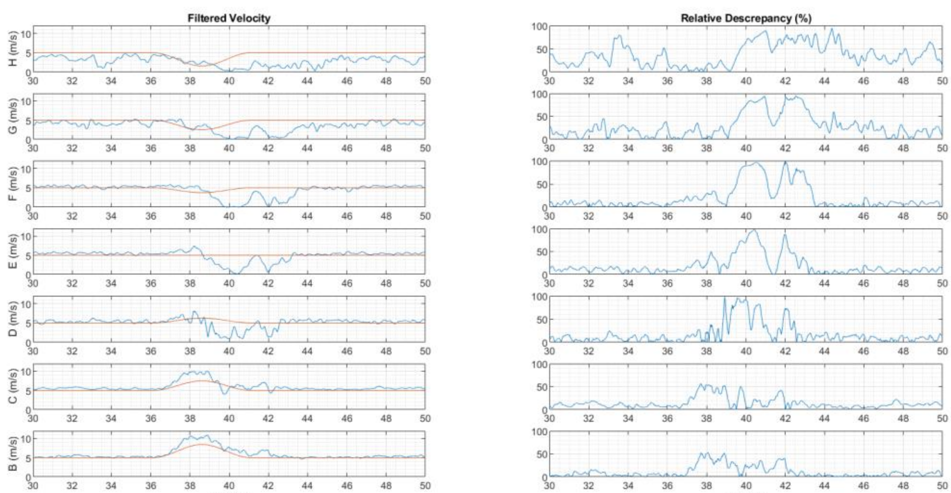

(c) negative EVS

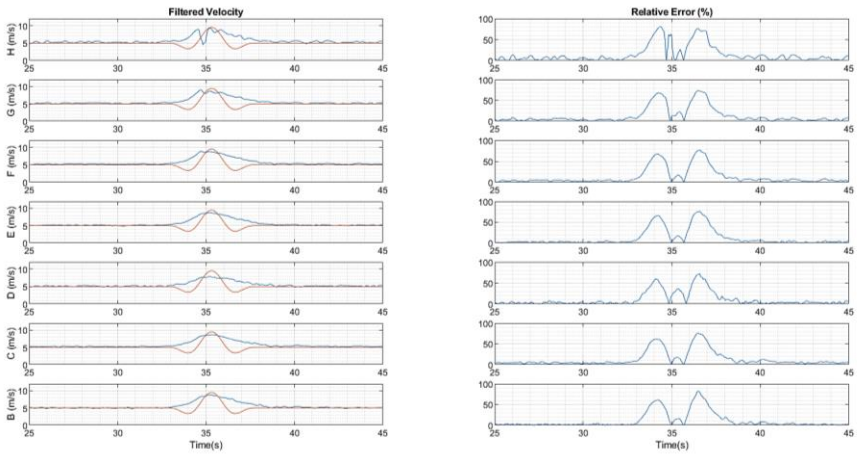

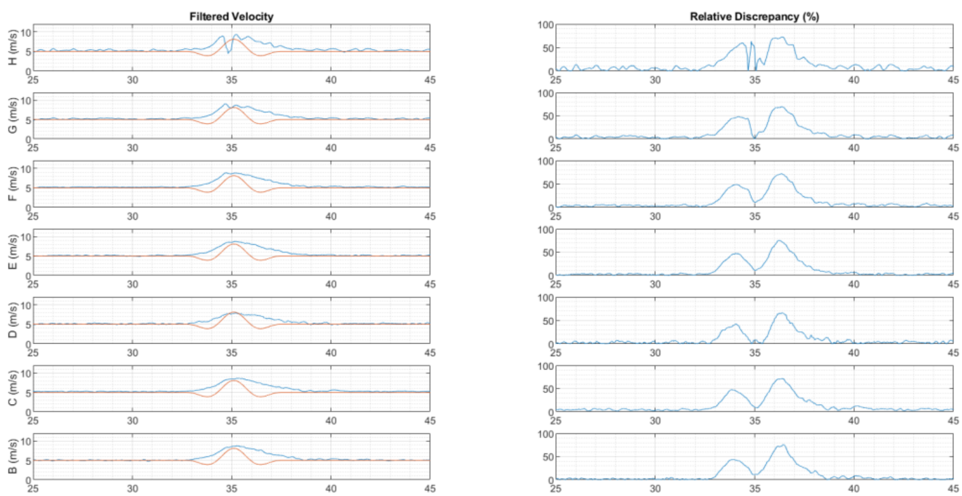

(d) EOG generated with changing fan powers, vertical measurements

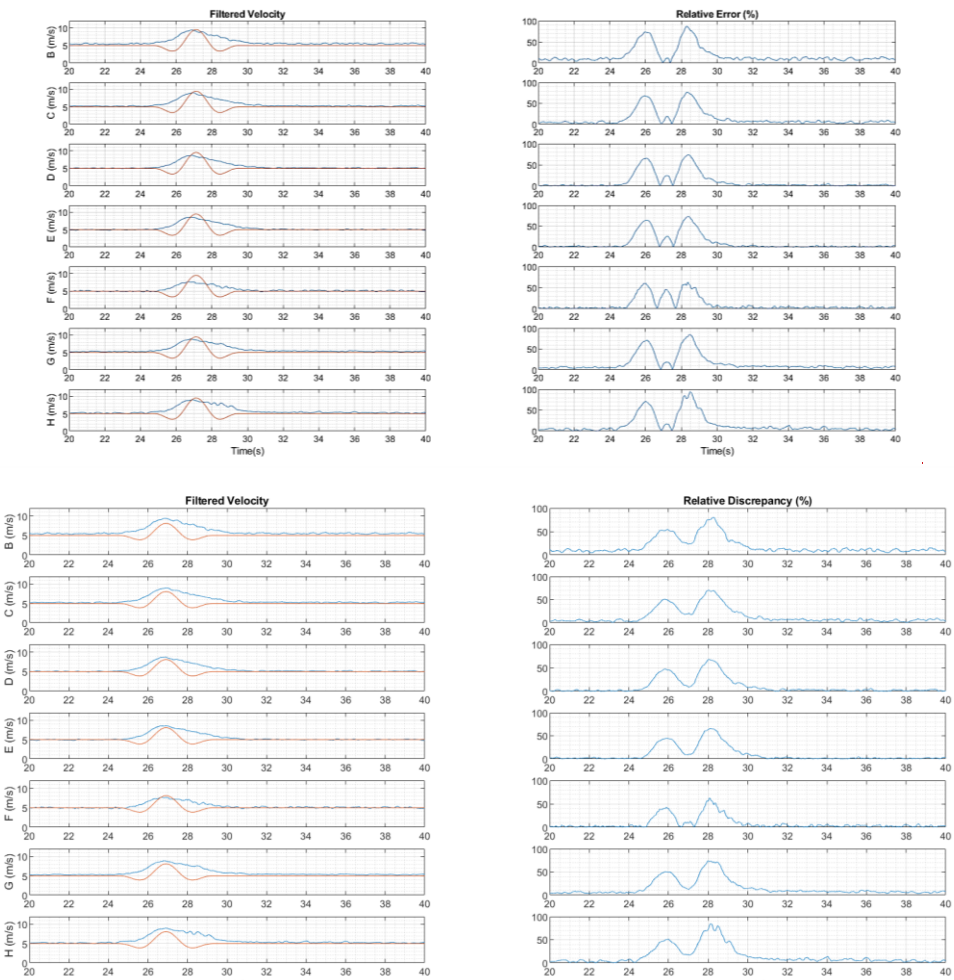

(e) EOG generated with changing fan powers, horizontal measurements

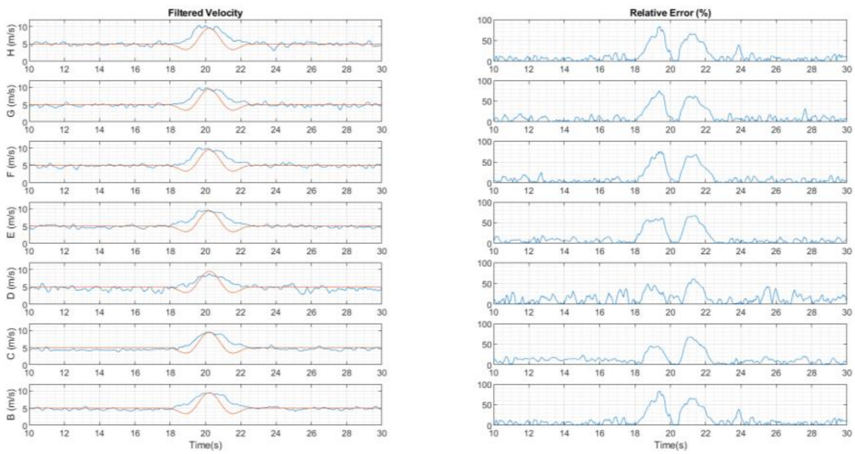

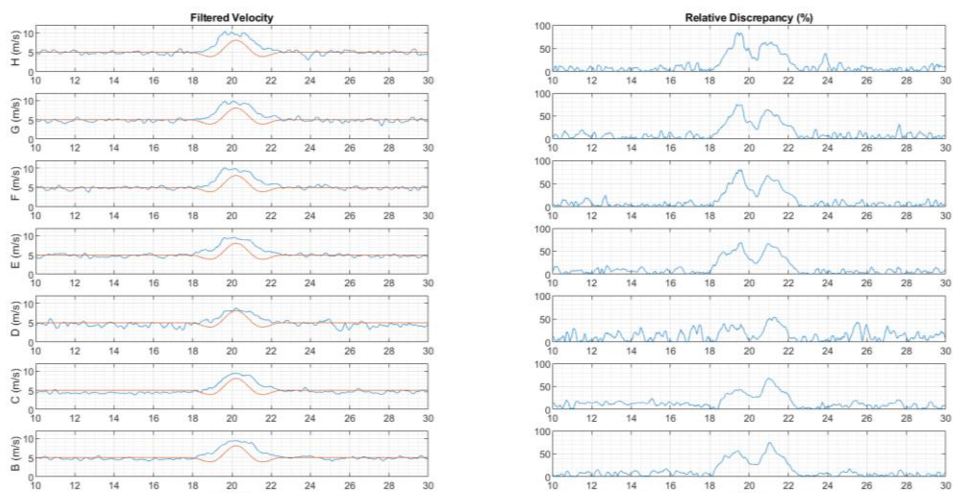

(f) EOG generated with IGVs, vertical measurements

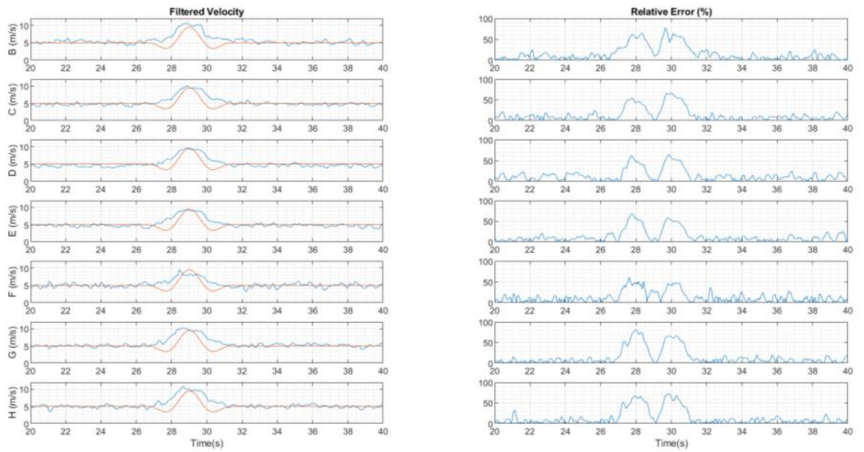

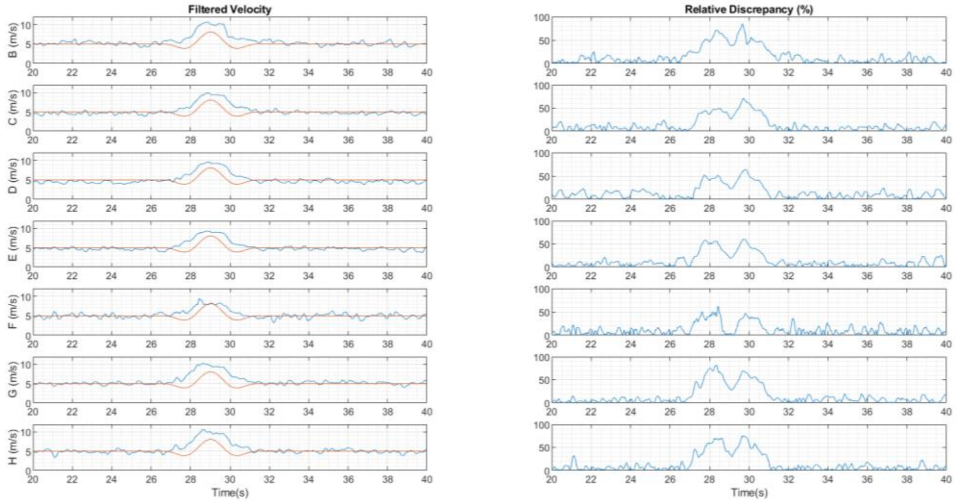

(g) EOG generated with IGVs, horizontal measurements

Figure 12. Filtred velocity time history at each probe (with the layout presented in Figure 6) as blue solid ~~blue~~ line compared with prescribed extreme event velocity as ~~a solid~~the orange solid line (left ~~column~~columns), time history of relative instantaneous velocity discrepancy normalized by average velocity (right ~~column~~columns)

The most consistent ~~uniform gust~~EOG was generated by using IGVs~~,~~ in terms of uniformity, symmetry and peak ~~factors~~factor at the test section~~, at least in the measurements area~~ (Figure 12f & g). The only noticeable ~~discrepancy for the EOG generated~~inconsistency of this simulated EOG with the ~~IGVs is due to~~IEC are the small ~~drop in~~ velocity ~~before and after the main rise of velocity in the prescribed gust case, which~~drops that created ~~dual peaks~~ a moderately symmetric double hump profile in the relative ~~error~~discrepancy time history. If we ~~consider~~considered the simplified gust profile as the baseline (see ~~Figure 9a~~Figure 8c), the generated gusts with this method would have ~~identical~~more similar characteristics ~~with~~to the theory.

4. Conclusion

A ~~numerical and~~hybrid experimental/numerical study has been carried out to investigate the possibility of creating extreme conditions for a scaled HAWT based on the IEC 61400-1 standard, in particular the EOG~~, EVS~~ and ~~EHS cases~~EWSs, using ~~the~~a unique 60 fan setup in the WindEEE dome~~.~~ at Western University. These conditions were tailored for a 2.2 m diameter ~~scaled~~test HAWT~~. The~~ with the aim ~~was~~ to further relate this work to full-scale wind turbines. Therefore, a ~~simple~~ length and time scaling approach based on tip vortex propagation in the wake was ~~presented. Based on that approach, the duration of each extreme condition was set equal to four tip vortex loops propagating downstream. Accordingly, the~~introduced. The resulting time scale is a function of the free stream velocity, tip speed ratio and diameter of the rotor.

~~The developed~~ A simplified numerical model ~~of the test chamber for 2D flow mode of operation gave a good understanding of the relation between fan power set point~~ was first developed and ~~the flow field in the relevant part of test chamber. This knowledge was successfully used to predict the fan setups to physically replicating the extreme conditions.~~

~~The~~ tuned based on a set of steady ~~experiment runs corresponding to the peak of the shear cases show the fans act non-linearly and they have different individual efficiencies, especially the top and bottom rows despite our simplified assumptions for developing the CFD~~ ABL flow data; the model~~. By knowing these discrepancies, corrections can be applied to the fan inputs for improving the accuracy with which the standard gust can be better replicated. The unsteady shear flow experiments showed that the flow field is more distorted due to the differences in speed generated at the fans. There is~~ used a ~~time lag between the highest and lowest peak location, which also can be corrected in future by giving a phase difference in actuations between the top and bottom rows. But more importantly the desired peak factor overall has been captured.~~

~~Generating uniform gusts using the IGVs produced the best results in terms of time scale and peak factors, as well as flow field uniformity. Considering the simplified gust profile without the velocity drops, the generated gust imitates the theoretical profile. The results from changing fan power set-points were consistent as well. However, due to flow recirculation and a sharp turn from the top and behind the fans, the top row of fans does not work as efficiently as the other 3 rows during large transitions in power set-points, which resulted on a little non-uniformity at top heights of the test chamber. The contraction walls when all 60 fans were operating helped unify the flow field, yet in high power transitions some intermittencies are noticeable at the top of the chamber. The same problem was mentioned for generating sheared flows.~~

~~Overall, this study demonstrated a successful simulation of extreme wind conditions, which can now be used for future experimental tests to investigate their effects on different aspects of wind turbine performance with minor modifications. It is informative to note again that the experiment results are directly from the prediction of the numerical model which had~~ simplified geometry of the WindEEE testing chamber and did not simulate the flow recirculation in the outer shell. The model also treated the fans simply as velocity inlet boundary conditions with the same efficiencies. Yet, it gave a good understanding of the relation between fan power set-points and the flow field at relevant part of the test chamber, which then was used to predict the fan setups for the physical simulation of the extreme events. For future target scenarios the numerical model can be useful to obtain the primary setup, however field adjustments are recommended.

Steady experiment runs corresponding to the peak of the shear cases showed that the fans act non-linearly having different individual efficiencies, especially the top and bottom rows due to the sharp recirculation angle at the suction side of the 60 fan wall. This has not been taken into account in the simplified CFD model and consequently resulted in discrepancies between experiments and the standard shear. By quantifying these discrepancies, corrections can be applied to improve the replication of these events. The unsteady shear flow experiments showed that even though the desired peak factor was generated the high and low velocity peaks reach the test section with a time lag. This can be corrected in the future by providing a phase difference in actuations between the top and bottom rows of fans.

In generation of the EOG by dynamic change of the fan powers, the flow field was more consistent than the EWS compared to their own baselines; the combination of 60 operating fans and the contraction walls helped unifying the flow field. Yet, in fast power transitions due to the sharp recirculation angle the flow field showed some unpredictability and inconsistency close to the ceiling of the test chamber. Generating uniform gusts using the IGVs produced the best results in terms of time scale and peak factor, as well as flow field uniformity and reproducibility. Considering the simplified gust profile without the velocity drops, the generated gust imitates the theoretical profile.

Overall, this study demonstrated promising results using a hybrid numerical/experimental approach for the simulation of extreme wind conditions. These extreme gust conditions can be used with minor modifications in future physical tests to investigate their effects on different aspects of wind turbines' performances. Furthermore, a detail investigation into the reproducibility of these extreme events, specifically the cases generated by dynamic change of the fan powers, is recommended.

Authors contributions

KS developed the numerical model and the scaling with direct supervision from CC. KS carried out all the experiments with supervision of HH. KS wrote the main body of the paper with input from all authors.

Competing interests

The authors declare that they have no conflict of interest

Acknowledgements

All authors thank Gerald Dafoe and Tristan Cormier for helping with the measurement setups. The present work is supported by the UWO, NSERC and the IESVic.

References

Anvari, M., Lohmann, G., Wächter, M., Milan, P., Lorenz, E., Heinemann, D., Tabar, M. R. R. and Peinke, J.: Short term fluctuations of wind and solar power systems, New J. Phys., 18(6), 063027, doi:10.1088/1367-2630/18/6/063027, 2016.

Bossanyi, E. A., Kumar, A. and Hugues-Salas, O.: Wind turbine control applications of turbine-mounted LIDAR, J. Phys. Conf. Ser., 555, 012011, doi:10.1088/1742-6596/555/1/012011, 2014.

Burton, T., Jenkins, N., Sharpe, D. and Bossanyi, E.: Wind Energy Handbook, 2nd ed., John Wiley and Sons Ltd, Chichester, UK., 2011.

Cheng, P. W. and Bierbooms, W. A. A. .: Distribution of extreme gust loads of wind turbines, J. Wind Eng. Ind. Aerodyn., 89(3), 309–324, doi:https://doi.org/10.1016/S0167-6105(00)00084-2, 2001.

Chowdhury, J., Chowdhury, J., Parvu, D., Karami, M. and Hangan, H.: Wind flow characteristics of a model downburst, in American Society of Mechanical Engineers, Fluids Engineering Division (Publication) FEDSM, vol. 1, American Society of Mechanical Engineers (ASME)., 2018.

Estanqueiro, A. I.: A dynamic wind generation model for power systems studies, IEEE Trans. Power Syst., 22(3), 920–928, doi:10.1109/TPWRS.2007.901654, 2007.

Gharali, K. and Johnson, D. A.: Effects of nonuniform incident velocity on a dynamic wind turbine airfoil, Wind Energy, 18(2), 237–251, doi:10.1002/we.1694, 2015.

González-Longatt, F., Wall, P. P. and Terzija, V.: Wake effect in wind farm performance: Steady-state and dynamic behavior, Renew. Energy, 39(1), 329–338, doi:10.1016/j.renene.2011.08.053, 2012.

Hangan, H., Refan, M., Jubayer, C., Parvu, D. and Kilpatrick, R.: Big data from big experiments. The WindEEE Dome, in Whither Turbulence and Big Data in the 21st Century?, pp. 215–230, Springer International Publishing., 2016.

Hangan, H., Refan, M., Jubayer, C., Romanic, D., Parvu, D., LoTufo, J. and Costache, A.: Novel techniques in wind engineering, J. Wind Eng. Ind. Aerodyn., 171, 12–33, doi:10.1016/j.jweia.2017.09.010, 2017.

Hansen, K. S. and Larsen, G. C.: Full scale experimental analysis of extreme coherent gust with wind direction changes (EOD), J. Phys. Conf. Ser., 75, 012055, doi:10.1088/1742-6596/75/1/012055, 2007.

Hansen, M. O.: Aerodynamics of wind turbines, Third ed., Routledge, Abingdon, UK., 2015.

Hu, W., Letson, F., Barthelmie, R. J. and Pryor, S. C.: Wind gust characterization at wind turbine relevant heights in moderately complex terrain, J. Appl. Meteorol. Climatol., 57(7), 1459–1476, doi:10.1175/JAMC-D-18-0040.1, 2018.

IEC: (International Electrotechnical Commission) IEC 61400-1: Wind turbines - Part 1: Design requirements, 3rd ed., Geneva, Switzerland., 2005.

IEC: (International Electrotechnical Commission) IEC 61400-1: Wind energy generation systems - Part 1: Design requirements, 4th ed., Geneva, Switzerland., 2019.

Jeong, M. S., Kim, S. W., Lee, I. and Yoo, S. J.: Wake impacts on aerodynamic and aeroelastic behaviors of a horizontal axis wind turbine blade for sheared and turbulent flow conditions, J. Fluids Struct., 50, 66–78, doi:10.1016/j.jfluidstructs.2014.06.016, 2014.

Lackner, M. A. and Van Kuik, G. A. M.: The performance of wind turbine smart rotor control approaches during extreme loads, J. Sol. Energy Eng. Trans. ASME, 132(1), 0110081–0110088, doi:10.1115/1.4000352, 2010.

Lancelot, P. M. G. J., Sodja, J., Werter, N. P. M. and De Breuker, R.: Design and testing of a low subsonic wind tunnel gust generator, Adv. Aircr. Spacecr. Sci., 4(2), 125–144, doi:10.12989/aas.2017.4.2.125, 2017.

Micallef, D. and Sant, T.: Rotor aerodynamics in sheared inflow: An analysis of out-of-plane bending moments, J. Phys. Conf. Ser., 1037, 022027, doi:10.1088/1742-6596/1037/2/022027, 2018.

Neunaber, I. and Braud, C.: Characterization of a new perturbation system for gust generation: The Chopper, Wind Energy Sci. Discuss., 1–17, doi:10.5194/wes-2019-107, 2020.

Pace, A., Johnson, K. and Wright, A.: Preventing wind turbine overspeed in highly turbulent wind events using disturbance accommodating control and light detection and ranging, Wind Energy, 18(2), 351–368, doi:10.1002/we.1705, 2015.

Petrović, V., Berger, F., Neuhaus, L., Hölling, M. and Kühn, M.: Wind tunnel setup for experimental validation of wind turbine control concepts under tailor-made reproducible wind conditions, in Journal of Physics: Conference Series, vol. 1222., 2019.

Refan, M. and Hangan, H.: Aerodynamic performance of a small horizontal axis wind turbine, J. Sol. Energy Eng. Trans. ASME, 134(2), doi:10.1115/1.4005751, 2012.

Ricci, S., De Gaspari, A., Riccobene, L. and Fonte, F.: Design and Wind Tunnel Test Validation of Gust Load Alleviation Systems, in 58th AIAA/ASCE/AHS/ASC Structures, Structural Dynamics, and Materials Conference, American Institute of Aeronautics and Astronautics, Reston, Virginia., 2017.

Schlipf, D., Schlipf, D. J. and Kühn, M.: Nonlinear model predictive control of wind turbines using LIDAR, Wind Energy, 16(7), 1107–1129, doi:10.1002/we.1533, 2013.

Sezer-Uzol, N. and Uzol, O.: Effect of steady and transient wind shear on the wake structure and performance of a horizontal axis wind turbine rotor, Wind Energy, 16(1), 1–17, doi:10.1002/we.514, 2013.

Shen, X., Zhu, X. and Du, Z.: Wind turbine aerodynamics and loads control in wind shear flow, Energy, 36(3), 1424–1434, doi:10.1016/j.energy.2011.01.028, 2011.

Snel, H., Schepers, J. G. and Montgomerie, B.: The MEXICO project (Model Experiments in Controlled Conditions): The database and first results of data processing and interpretation, in Journal of Physics: Conference Series, vol. 75., 2007.

Sørensen, N. N., Michelsen, J. A. and Schreck, S.: Navier-Stokes predictions of the NREL phase VI rotor in the NASA Ames 80 ft × 120 ft wind tunnel, Wind Energy, 5(2–3), 151–169, doi:10.1002/we.64, 2002.

Suomi, I., Vihma, T., Gryning, S.-E. and Fortelius, C.: Wind-gust parametrizations at heights relevant for wind energy: a study based on mast observations, Q. J. R. Meteorol. Soc., 139(674), 1298–1310, doi:10.1002/qj.2039, 2013.

TFI Ltd.: Cobra Probe, Turbul. Flow Instrum. Pty Ltd [online] Available from: https://www.turbulentflow.com.au/Products/CobraProbe/CobraProbe.php (Accessed 12 June 2020), 2011.

Thomsen, K. and Sørensen, P.: Fatigue loads for wind turbines operating in wakes, J. Wind Eng. Ind. Aerodyn., 80(1–2), 121–136, doi:10.1016/S0167-6105(98)00194-9, 1999.

Ueckerdt, F., Hirth, L., Luderer, G. and Edenhofer, O.: System LCOE: What are the costs of variable renewables?, Energy, 63, 61–75, doi:10.1016/j.energy.2013.10.072, 2013.

Wächter, M., Heißelmann, H., Hölling, M., Morales, A., Milan, P., Mücke, T., Peinke, J., Reinke, N. and Rinn, P.: The turbulent nature of the atmospheric boundary layer and its impact on the wind energy conversion process, J. Turbul., 13, 1–21, doi:10.1080/14685248.2012.696118, 2012.

Wester, T. T. B., Kampers, G., Gülker, G., Peinke, J., Cordes, U., Tropea, C. and Hölling, M.: High speed PIV measurements of an adaptive camber airfoil under highly gusty inflow conditions, J. Phys. Conf. Ser., 1037, 072007, doi:10.1088/1742-6596/1037/7/072007, 2018.